Technical Report 1235

Passive and Active Grasping with a Prehensile Robot End-Effector

Helen Greiner

MIT Artificial Intelligence Laboratory

REPORT DOCUMENTATION PAGE		READ INSTRUCTIONS BEFORE COMPLETING FORM
1 REPORT NUMBER AI-TR 1235	2 GOVT ACCESSION NO	3 RECIPIENT'S CATALOG NUMBER
4 TITLE (and Subtitle) Passive and Active Grasping with a Prehensile Robot End-Effector		5 TYPE OF REPORT & PERIOD COVERED technical report 6 PERFORMING ORG REPORT NUMBER
7 AUTHOR(s) Helen Greiner		8 CONTRACT OR GRANT NUMBER(s) 291-CE-505-0-3470 N00014-86-K-0685
9 PERFORMING ORGANIZATION NAME AND ADDRESS Artificial Intelligence Laboratory 545 Technology Square Cambridge, MA 02139		10 PROGRAM ELEMENT, PROJECT, TASK AREA & WORK UNIT NUMBERS
11 CONTROLLING OFFICE NAME AND ADDRESS Advanced Research Projects Agency 1400 Wilson Blvd. Arlington, VA 22209		12 REPORT DATE May 1990 13 NUMBER OF PAGES 72
14 MONITORING AGENCY NAME & ADDRESS(if different from Controlling Office) Office of Naval Research Information Systems Arlington, VA 22217		15 SECURITY CLASS (of this report) UNCLASSIFIED 15a DECLASSIFICATION/DOWNGRADING SCHEDULE

16 DISTRIBUTION STATEMENT (of this Report)

Distribution is unlimited

17 DISTRIBUTION STATEMENT (of the abstract entered in Block 20, if different from Report)

18 SUPPLEMENTARY NOTES

None

19 KEY WORDS (Continue on reverse side if necessary and identify by block number)

gripper
prehensile
compliant
passive
behavior
touch sensing

20 ABSTRACT (Continue on reverse side if necessary and identify by block number)

This report presents a design of a new type of robot end-effector with inherent mechanical grasping capabilities. Concentrating on designing an end-effector to grasp a simple class of objects, cylindrical, allowed a design with only one degree of actuation. The key features of this design are high bandwidth response to forces, passive grasping capabilities, ease of control, and ability to wrap around objects

(con.t on back)

(block 20 con't)

with simple geometries providing form closure. A prototype of this mechanism was built to evaluate these features.

Passive and Active Grasping with a Prehensile Robot End-Effector

by

Helen Greiner

Submitted to the
Department of Electrical Engineering and Computer Science
in Partial Fulfillment of the Requirements for the
Degree of Master of Science

at the
Massachusetts Institute of Technology

May, 1990

Passive and Active Grasping with a Prehensile Robot End-Effector

by

Helen Greiner

Abstract

This report presents a design of a new type of robot end-effector with inherent mechanical grasping capabilities. Concentrating on designing an end-effector to grasp a simple class of objects, cylindrical, allowed a design with only one degree of actuation. The key features of this design are high bandwidth response to forces, passive grasping capabilities, ease of control, and ability to wrap around objects with simple geometries providing form closure. A prototype of this mechanism was built to evaluate these features.

Thesis Supervisor: J. Kenneth Salisbury
Title: Research Scientist, MIT AI Laboratory

Acknowledgements

This work was performed in cooperation with the Jet Propulsion Laboratory through the MIT Engineering Internship Program. I would like to thank the Tele-Autonomous Systems Group at JPL for encouraging this work even though it differed from their usual direction of research. Special thanks to my supervisor Henry Stone for encouraging and supporting this project, Zoltan Szakaly for practical engineering advice, Hemanshu Lakhani for many shared experience at JPL, and Timothy Ohm for providing some of the illustrations.

I was extremely fortunate to be able to spend part of my graduate school experience in the MIT Artificial Intelligence Laboratory. Thanks to all the people who help make it an interesting, creative and fun place to do research. Thanks especially to Colin Angle for taking the photographs, also David Siegel and Dave Barrett for proofreading the draft of this work. Most of all I would like to thank my advisor, Ken Salisbury, who helped me coordinate a project of interest to both JPL and MIT.

This research was performed at both the MIT Artificial Intelligence Laboratory and NASA's Jet Propulsion Laboratory. At JPL, the research was funded by the Tele-Autonomous Systems Section under JPL charge number 291-CE-505-0-3470. Support at the MIT Artificial Intelligence Laboratory was provided, in part, by the University Research Initiative under Office of Naval research contract N00014-86-K-0685.

Contents

List of Figures

Chapter 1

Introduction

1.1 Project Motivation

Robots are typically equiped with end-effectors which can secure and hold selected objects tightly. A robot end-effector can be designed to incorporate many degrees of freedom which increases complexity of planning and control, or it can be designed with fewer degrees of freedom which limits its capabilities but simplifies its operation.

A robot end-effector with the latter characteristics is needed by NASA for robotic truss acquisition and assembly. An end-effector such as this would not be used to grasp a wide range of distinct objects. Therefore, I have chosen to concentrate on an end effector designed specifically to grasp a simple class of objects, in this case cylindrical.

1.2 Design Discussion

Robots typically have very rigid links and transmissions. This creates problems when they come into contact with a rigid environment. If the robots have no compliance, small motions in the wrong direction can cause serious damage. Active force control strategies can be used but they are bandwidth limited and tend to be

unstable when contacting rigid objects.

Recently, however, there has been a thrust toward making robots more responsive to tasks they perform and their environments. In the WAM Arm [1], for example, a backdrivable transmission allows safe collisions, lightweight carbon fiber links are used for low inertia, and the links are covered with a foam material. The key element of the design is that the force control ability is inherent in the mechanism making it naturally better at interacting with its environment.

This report extends this idea to end-effector design. End-effectors that come into contact frequently with the environment should be compliant. Analysis, design, and evaluation of such an end-effector is presented in this document. The mechanism is refered to as a **P**rehensile [1] **A**cquisition **L**inkage **M**echanism, or **PALM**. Much the same as prehensile grasping in monkeys, the **PALM** is designed to grasp objects rapidly from one side.

This device has one active and two passive degrees of freedom. Analysis of the kinematics led to a design which includes three joints, three links, and a particular ratio of link lengths. An important and novel aspect of the device is that it exhibits both active and passive grasping capabilities. A tendon drive mechanism transmits actuation forces to the joints allowing active control. The same mechanism allows the **PALM** to passively curl in response to a force applied to any of its links. One advantage to such a design is a high bandwidth response to forces, and consequently a high gripping speed. Designing an active control system to achieve this type of response would be difficult if not impossible.

1.3 Previous Work

Several types of one degree-of-freedom gripping devices have been developed to mount on robot end plates. The most common are one degree-of-freedom parallel

[1] Prehensile - adapted for seizing or grasping esp. by wrapping around

jaw grippers. However, these grippers have limited capabilities and work best with rectangular objects or objects for which custom fingers have been designed. Alternatively, the fingers can incorporate several degrees of freedom in a serial linkage [7]. These fingers have increased capabitities, but coordination and control is more difficult.

To perform simple tasks, in many cases the best control scheme is simply to wrap about an object until contact occurs on each segment of the gripper. The behavior of fingers with a serial linkage can be modified to have only one active degree-of-freedom by coupling two or more joints. This suggests a unique category of end-effectors called curling fingers.

A variety of mechanisms have been designed to obtain curling behavior. This project builds upon several important design concepts as described below. A few researchers have investigated the use of pulleys in coupling joint motions in grippers. Sukhan Lee [3] has investigated a dexterous hand with 14 joints controlled by eight motors. In his design the finger joints are coupled by pulleys. Hirose [2] has developed a one degree-of-freedom "soft gripper" consisting of a number of links coupled by pulleys. This mechanism is designed to conform to an object and hold it with a uniform pressure distribution. The pulley system which the **PALM** uses to transmit the gripping force is similar to these two designs. The major difference between the two is the method of selecting the torque distribution in the joints. Rovetta and Casarico [6] have constructed a two-fingered mechanical hand which contains linkages connected with wires and return springs. These springs allow the designers to dictate the sequential motions of the linkages, and return the links back to their resting position. Similarly, the **PALM** design incorporates springs placed between the joints which resolve the kinematic indeterminacies in the system, they also function to spring center the device and to compensate for the weight of the device when it is in the horizontal position.

Chapter 2

Analysis

2.1 Kinematics

The following kinematic analysis was used to determine the relevant dimensions of the **PALM**. One possible criteria for a grasp is that it must provide *form closure* whereby the resultant of the non-friction dependent forces applied by any combination of links must oppose the resultant of the others. In other words, the grasped object is completely restrained. Alternatively, a *force closure* grasp can resist only some disturbance forces [7]. Form closure was selected as a criterion for a *good* grasp. It provides a more secure grasp than force closure because it does not rely upon friction. Form closure grasps are discussed further in Section 2.2 where the workspace of the **PALM** is analyzed. This section relates how the ratio of link lengths was selected based on the form closure criterion.

2.1.1 Model

To provide the minimum number of point contacts needed for form closure about a cylinder, the mechanism must have three links. The **PALM** is designed to be mounted to a robot end-effector making only two joints necessary. However, three

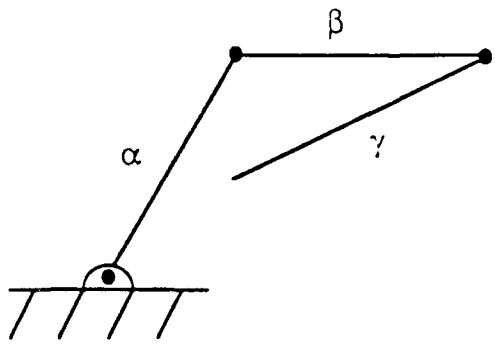

Figure 2.1: Link Terminology. Proximal link - α. Central Link - β. Distal Link - γ.

joints are included which increases **PALM**'s workspace and consequently increases the allowable positioning error for the robot. To improve the clarity of the following discussion of the kinematics, we define the terminology shown in Figure 2.1 where the proximal, central, and distal link lengths are labelled α, β, and γ, respectively.

2.1.2 Range of Cylinder Diameters

The range of cylinder diameters which can be held in form closure was characterized for a planar three link mechanism. If the total length of the mechanism is normalized (i.e. $\alpha + \beta + \gamma = 1$), two independent parameters (two dimensionless link lengths) can be used to describe the system. The normalized ratios α and β were arbitrarily chosen as the independent parameters describing the system. Figure 2.2 shows the range of cylinder diameters which can be held in form closure as a function of these two parameters. The point on the figure which maximizes this range of cylinders is at the intersection of the central bold lines. Here the ratio of link lengths is 0.25 : 0.5 : 0.25, and the diameter of cylinders that can be grasped ranges from zero to half the total length of the mechanism. However, with this ratio of link lengths,

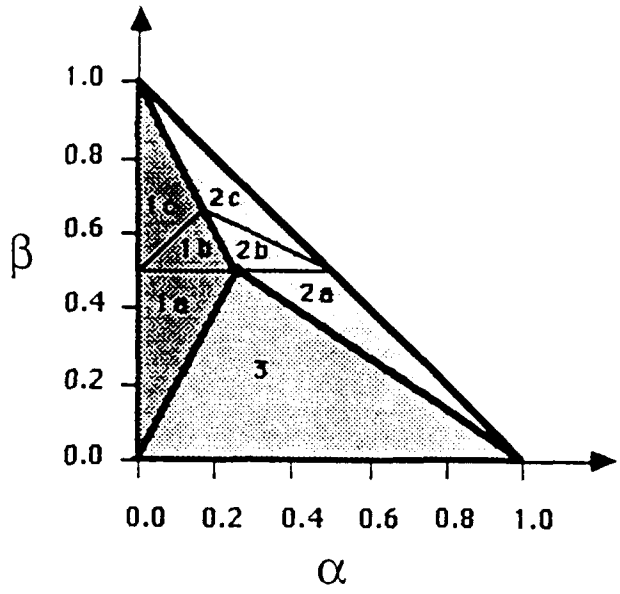

Figure 2.2: Range of Diameters that Can be Held in Form Closure. The range of diameters which can be grasped in each area of the graph are: 1a) $0 < d < 2\alpha$, 1b) $\beta - \alpha - \gamma < d < 2\alpha$, 1c) no diameters, 2a) $0 < d < 2\gamma$, 2c) no diameters, 3) $0 < d < \beta$

the maximum and minimum diameters can only be grasped in one form closure configuration (see Figure 2.3). To grasp these two extremes, the end effector would have to be positioned with great accuracy with respect to the cylinder because the contact point is at the joint axis. Also, the first link can not independently apply a normal force to the cylinder. Therefore, an additional criterion was established, namely that of maximizing the range of possible link configurations which results in distinct form closure solutions.

2.1.3 Range of Link Configurations

A dimensionless quantity, s, was introduced to quantify the range of possible link configurations (see Figure 2.4). For a normalized total length ($\alpha + \beta + \gamma = 1$), s is defined as the distance along the central link that a point on the cylinder can slide. It is important to notice that the value of s is a function of the diameter

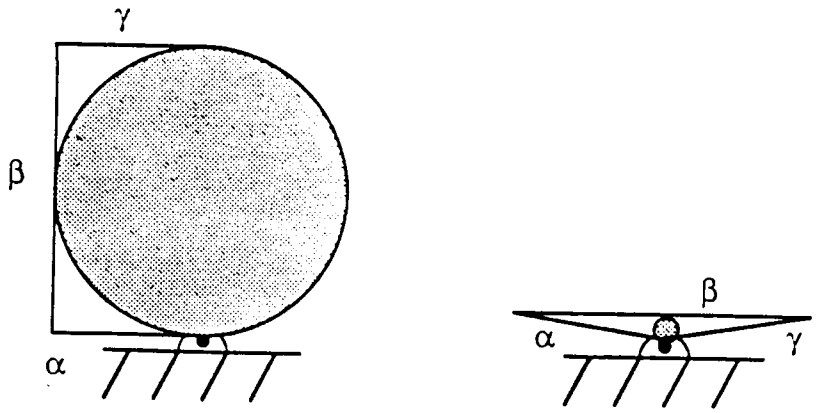

Figure 2.3: Grasps at Extremes of Range of Diameters

of the cylinder, d. The value of this quantity is characterized in terms of the link parameters for small diameter cylinders in Figure 2.5. The maximum range of link configurations corresponds to the intersection of the central bold lines as before. At this point, all the links are equal in length. For other diameters, the shape of this space is similar but the intersection of the lines is shifted and the value of s is a more complex function of the link parameters and cylinder radius.

2.1.4 Compromise between Criteria

In order to increase the area in which a successful grasp can be accomplished, the proximal link should be as long as possible. This added criterion allowed an acceptable tradeoff between range of diameters and range of link configurations to be selected. A solution at the intersection of the line between sections 2a and 3 in Figure 2.2 and the line between sections 4 and 5 in Figure 2.4 was chosen. This point achieves the desired objective of having a large proximal link, and it is close to both the maximum range of diameters and the maximum range of link configurations. The normalized link ratios at this point are $\alpha : \beta : \gamma = 0.4 : 0.4 : 0.2$. A stick model

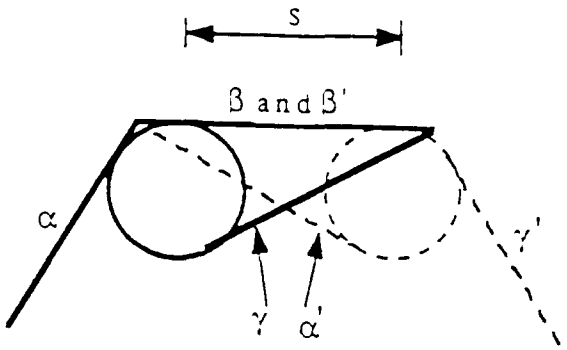

Figure 2.4: Range of Link Configurations Parameterized by s. The links labelled α, β, and γ show the link positions with cylinder at one extreme of motion. Likewise, the links labelled α', β', and γ' show the link positions with cylinder at the other extreme.

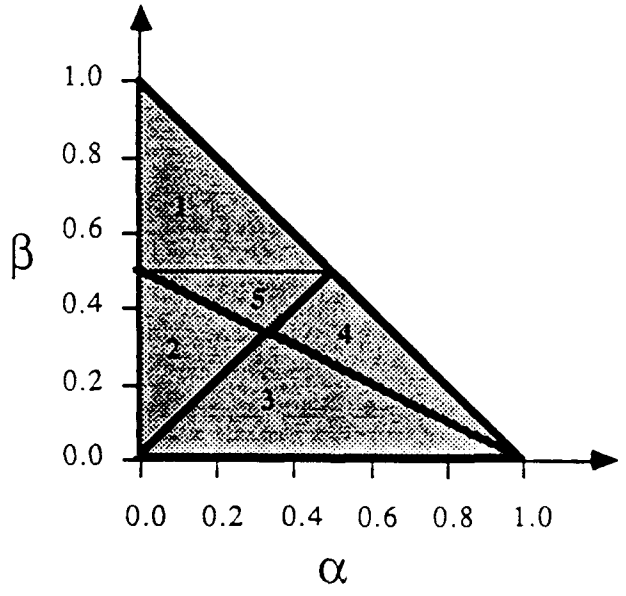

Figure 2.5: Range of Link Configurations Characterized for Cylinders with Small Diameters, ϵ. The areas in the graph are: 1) no grasp, 2) s=α, 3) s=β, 4) s=γ, 5) s=$\alpha + \gamma - \beta$.

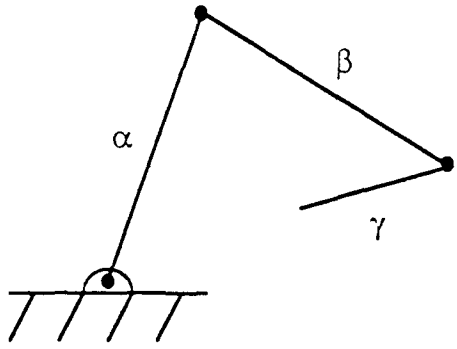

Figure 2.6: Model of Palm with Selected Ratio of Link Lengths (i.e. $\alpha : \beta : \gamma =$ 0.4:0.4:0.2)

of the **PALM** with these ratios is shown in Figure 2.6.

2.2 Workspace

An important consideration in evaluating the kinematic parameters of any gripper is the size of the workspace that they provide. For the pupose of this discussion, the workspace is divided into two types, the primary workspace and the secondary workspace. The primary workspace of the **PALM** is the area in which a fixed cylinder can be located such that a form closure grasp is possible. This will be described below by first analyzing a stick figure gripper, then extending the analysis to a geometric figure of **PALM**. The secondary workspace is the area in which a cylinder can be grasped, but the grasp does not provide form closure. In other words, grasps in the secondary workspace rely on friction contact between the cylinder and the links.

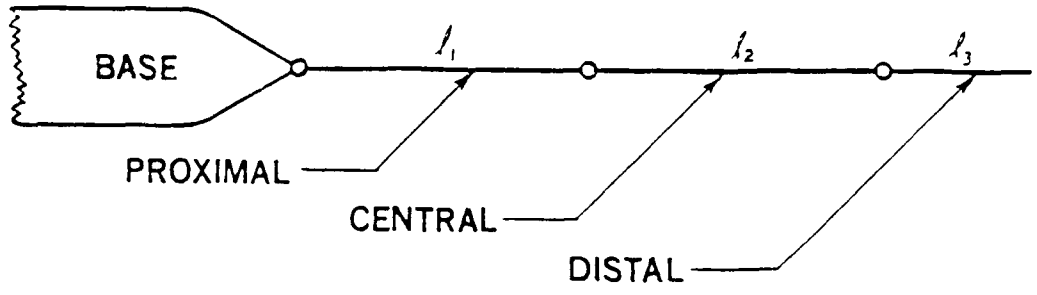

Figure 2.7: Stick Figure Gripper

2.2.1 Primary Workspace

For a stick gripper with the link parameters shown in Figure 2.7, the primary workspace can be calculated by finding the range on the proximal link that the cylinder must contact in order to achieve a form closure solution. If contact is made outside of this range, a grasp may still be possible, but it will fall in the secondary workspace.

To find this range, we will first establish the criterion for a form closure grasp as a function of the link parameters and cylinder radius. The two extrema of this range occur when the proximal and distal links are parallel, as shown in Figure 2.8. The two distances along the proximal link where this parallel condition holds are given in Equations 2.1 and 2.2.

$$x' = l_1 - \frac{l_2}{2}\left(1 - \sqrt{1 - \left(\frac{2r}{l_2}\right)^2}\right) \tag{2.1}$$

$$x = l_1 - \frac{l_2}{2}\left(1 + \sqrt{1 - \left(\frac{2r}{l_2}\right)^2}\right) \tag{2.2}$$

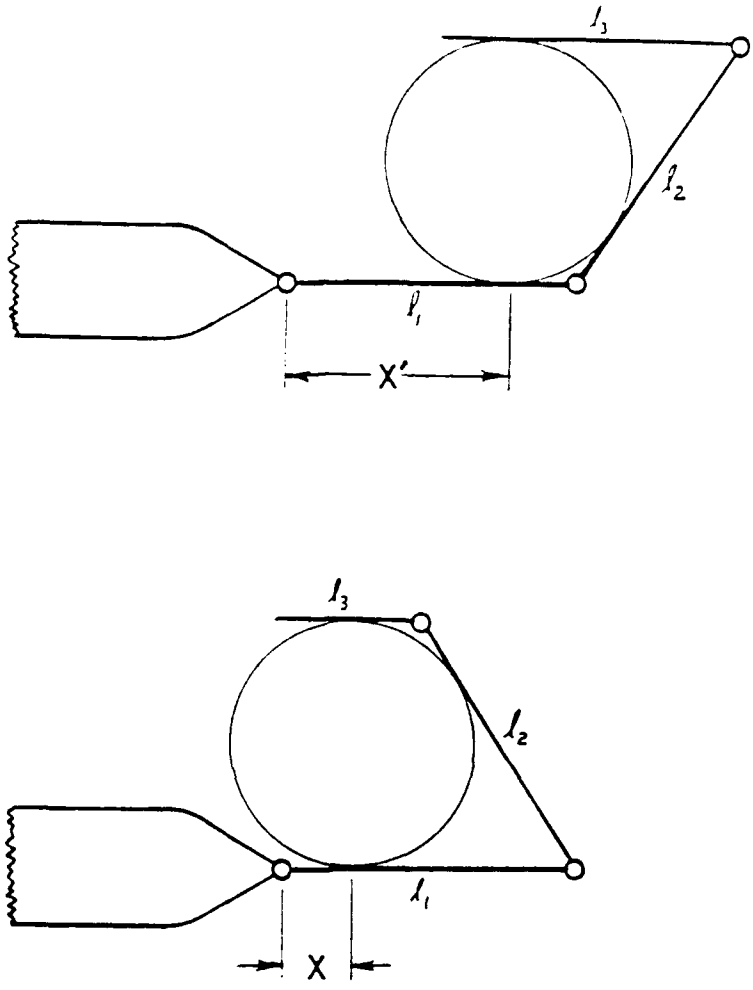

Figure 2.8: Limits of Form Closure Grasp. Proximal and distal links are parallel in each case.

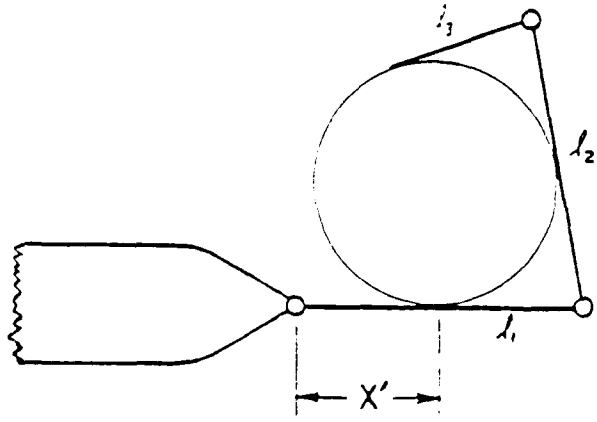

Figure 2.9: Tangential Contact Between Tip of Distal Link and Cylinder

These two conditions are not the only criterion for a form closure grasp. The distal link must also maintain tangential contact with the cylinder for a three contact grasp. The upper extreme on the range of grasps can occur when the very tip of the distal link contacts the cylinder (see Figure 2.9). This condition limits the upper extreme of the range, x'.

$$x' = l_1 - (l_2 - l_3) \tag{2.3}$$

These conditions can be combined to define the primary workspace. The upper extreme of the range is found from Equations 2.1 and Equation 2.3. By equating x' as derived by each of these two equations, we find that Equation 2.1 holds for cylinders where $r > \sqrt{l_3(l_2 - l_3)}$ and Equation 2.3 holds for cylinders where $r < \sqrt{l_3(l_2 - l_3)}$. With the kinematics described in the previous section, $l_1 = l_2 = 2l_3$, comparing the radius of cylinder, r, to l_3 determines which equation holds. However, if the radius, r, is greater than l_3, no form closure solution exists anyway. Therefore, the upper extreme of the primary workspace is found from Equation 2.3. The lower extreme of the primary workspace is found simply from Equation 2.2.

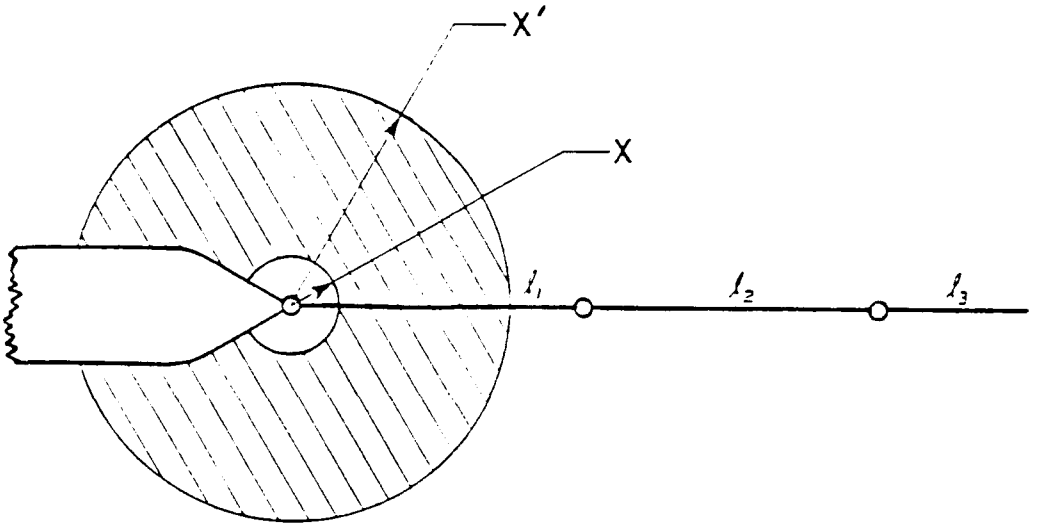

Figure 2.10: Workspace for Stick Gripper. The inner boundary is denoted by x and the outer boundary is denoted by x'.

An annulus is formed by rotating x' and x about the first joint. This annulus shown in Figure 2.10 is the primary workspace for the stick figure gripper. For a cylinder whose radius is equal to the length of the distal link, the primary workspace consists of only an arc because x' and x are equal. For a cylinder whose diameter is small, x approaches zero and the workspace is the area of the circle swept out by x'.

Now, we extend this analysis to consider the actual geometry of the **PALM** which is illustrated in Figure 2.11. The tapering of the links adds complexity to the equations derived to characterize the primary workspace. Again, we solve for the range of contacts that allow a form closure grasp. The same conditions as above are used to solve for x and x':

if $r < \sqrt{l_3(l_2 - l_3)}$

$$x' = \sqrt{r_{t1}^2 + (l_{t1} - l_{t2} + l_{t3})^2} \tag{2.4}$$

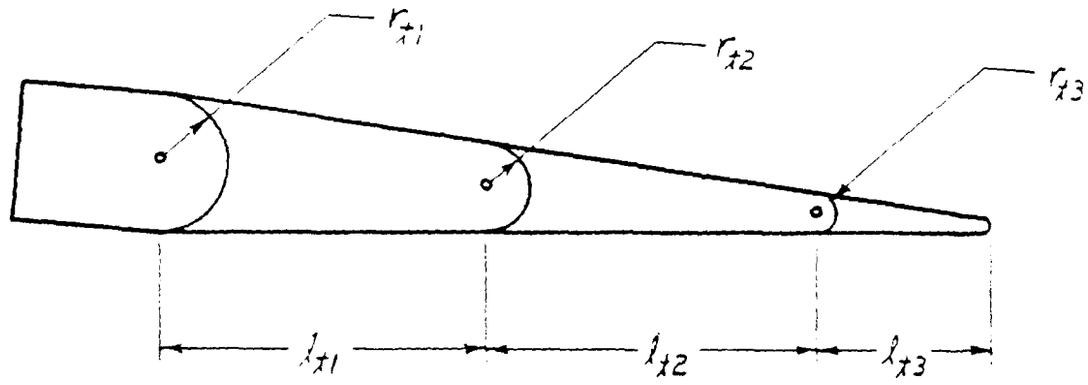

Figure 2.11: Geometry of **PALM**

else

$$x' = \sqrt{r_{t1}^2 + \left(l_{t1} - \frac{l_{t2}}{2}\left(1 + \sqrt{1 - \left(\frac{2r}{l_{t2}}\right)^2}\right)\right)^2} \tag{2.5}$$

$$x = \sqrt{r_1^2 + \left(l_{t1} - \frac{l_{t2}}{2}\left(1 + \sqrt{1 - \left(\frac{2r}{l_{t2}}\right)^2}\right)\right)^2} \tag{2.6}$$

Figure 2.12 shows the section of the annulus formed by x and x' which is the workspace for the **PALM**. Mechanical stops on the first joint of the **PALM** limit the workspace. Since the gripper is bidirectional, the workspace is symmetric on either side.

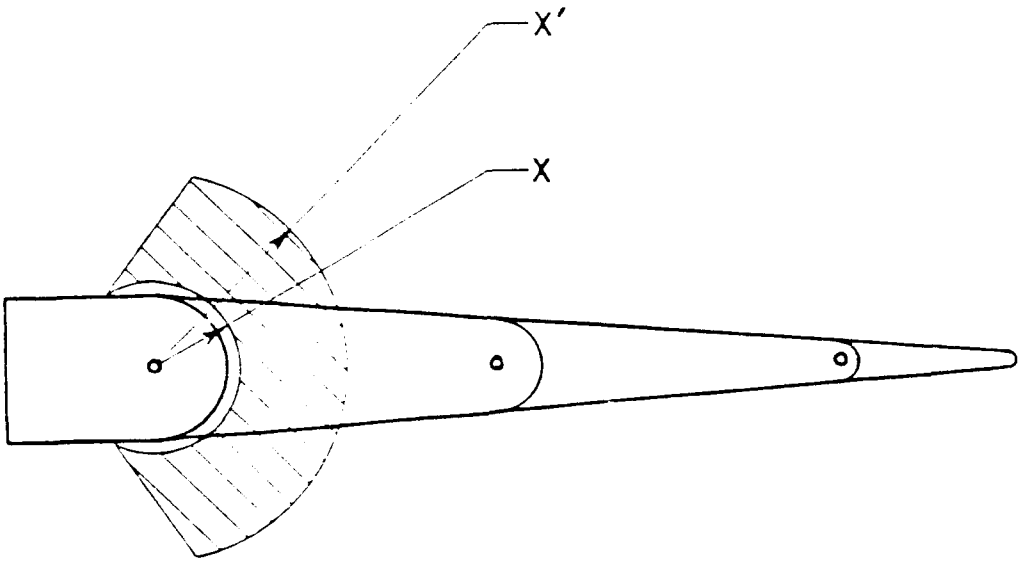

Figure 2.12: Workspace for **PALM**

2.2.2 Secondary Workspace

Grasps in the secondary workspace can have either two or three contacts between cylinder and gripper (illustrated in Figure 2.13). These grasps are not as desirable as grasps in the primary workspace because they rely on both friction and the forces that the links exert to hold the cylinder. The most important of these grasps is the "fingertip grasp" (Figure 2.13 C). This type of grasp extends the workspace of the **PALM** considerably, and can be used to draw objects into a better grasp.

The secondary workspace is difficult to quantify. If the coefficient of friction is large, the secondary workspace is approximately a disk which includes the primary workspace with outer radius equal to the length of the first two links, $l_1 + l_2$ (see Figure 2.14).

In demonstrating the prototype **PALM**'s ability to grasp cylinders of various sizes the secondary workspace was frequently used. The gripper tends to draw objects into form closure grasps, discussed in detail in Section 2.4. This characteristic gives the **PALM** a large useful workspace.

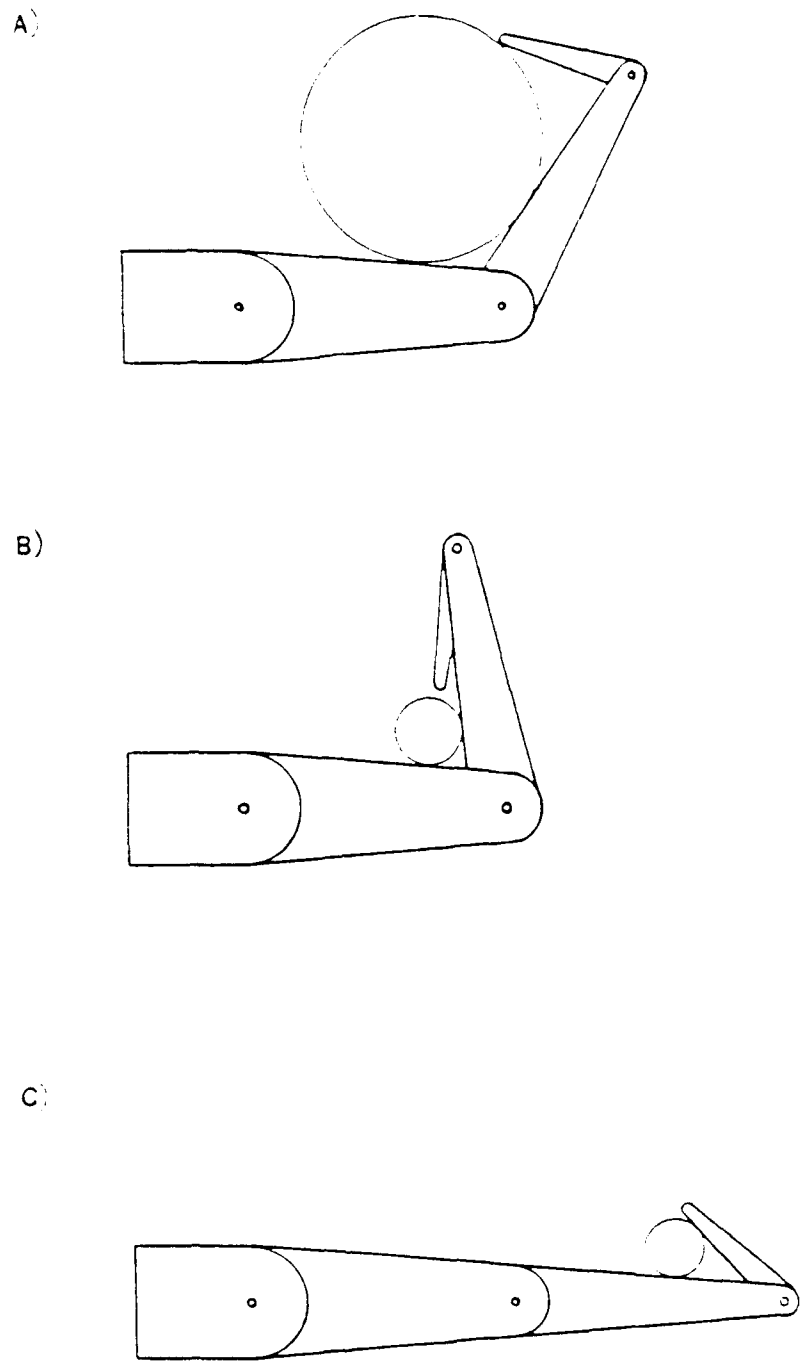

Figure 2.13: Examples of Grasps in the Secondary Workspace. A) 3 contact force closure, B) 2 contact force closure using proximal and central links. C) "fingertip grasp" - 2 contact force closure using central and distal links.

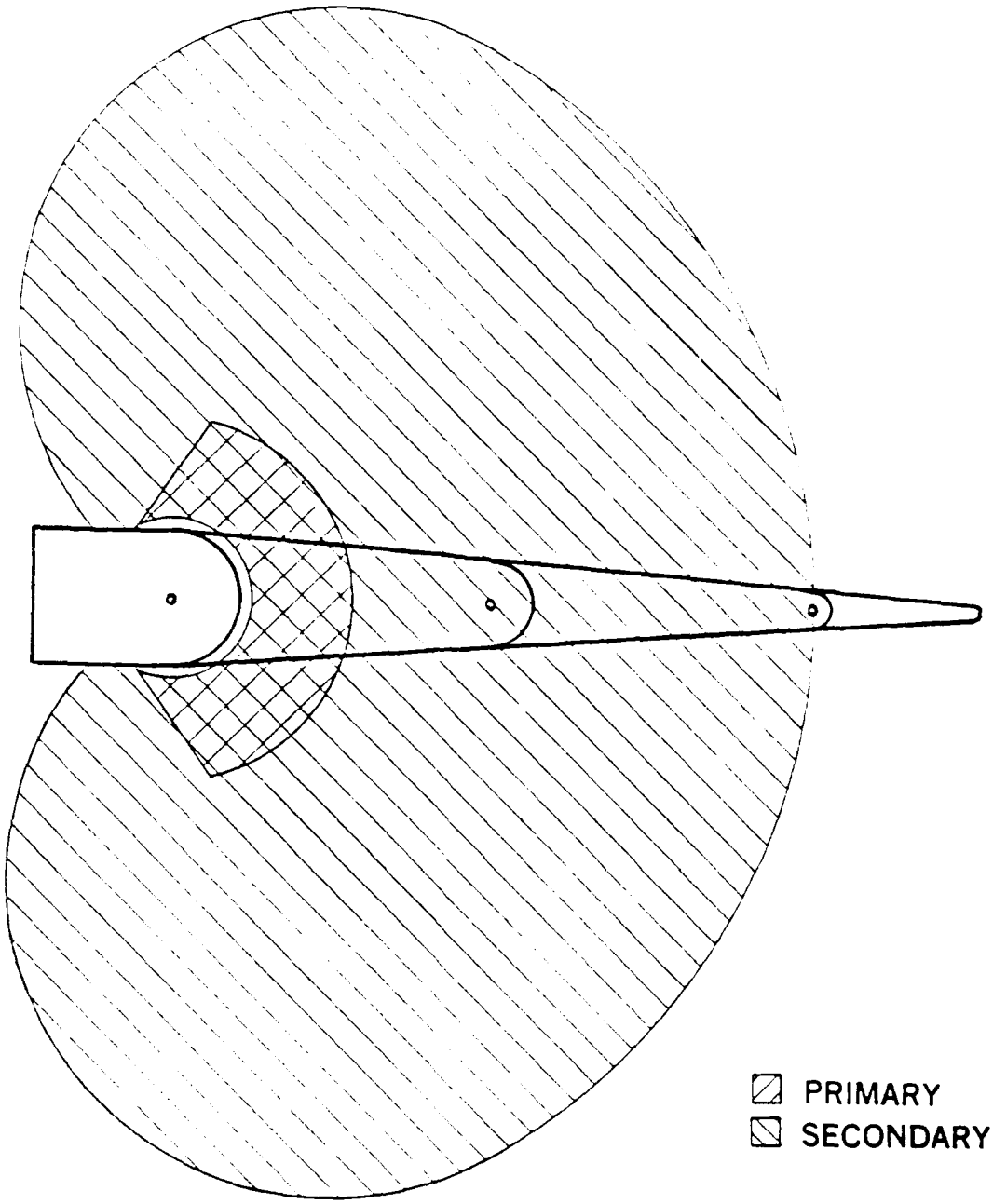

Figure 2.14: Approximate Secondary Workspace for a Fixed Cylinder and Large Coefficients of Friction at Contact

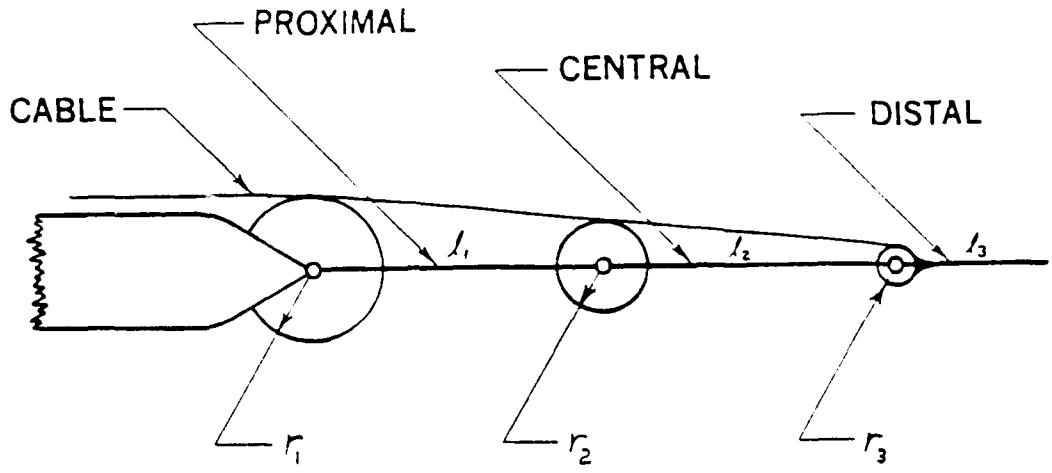

Figure 2.15: Model of PALM

2.3 Mechanical Behavior

In this section, important aspects of the mechanical behavior of the **PALM** are described. Information presented here is closely coupled to that in Section 3.1 which describes the mechanical design. At this point the reader is asked to ignore implementation issues. The following discussion uses the model shown in Figure 2.15. In this model, idler pullies rotate about the first two joints, and a pulley rotates about the third joint while rigidly attached to the distal link. This section first describes the criterion for choosing the ratio of pulley radii. Then, the gripper motion during active grasping is discussed. In the final section, the concept of passive grasping is introduced and the behavior is analyzed.

2.3.1 Dimensions

The device is designed to remain in static equilibrium when a force acts at the tip as shown in Figure 2.16. This behavior is accomplished through an appropriate combination of pulley ratios and link lengths (i.e., $\frac{l_3}{r_3} = \frac{l_2+l_3}{r_2} = \frac{l_1+l_2+l_3}{r_1}$). We define

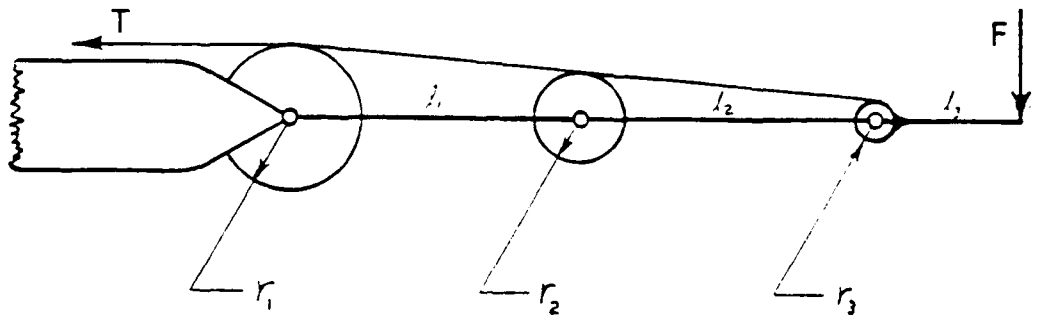

Figure 2.16: PALM in Equilibrium. The force is applied to the tip of the distal link.

the *aspect ratio* as the ratio of the grippers total length to half the width of its base ($\frac{l_1+l_2+l_3}{r_1}$=aspect ratio). The aspect ratio also gives the ratio of the tension in the cable to the magnitude of a force applied to the tip ($\frac{T}{F}$=aspect ratio). A small aspect ratio decreases the workspace, while a large aspect ratio decreases the force the gripper can supply at the tip. The aspect ratio was chosen on the basis of functionality and aesthetics to be 12:1. The ratio of pulley radii and link lengths plays an important part in dictating the mechanical behavior during both active and passive grasping as described in the next two sections.

2.3.2 Active Grasping

Active grasping involves rotating the joints such that they provide a form closure grasp about the cylinder. The simple algorithm that is used to have the **PALM** grasp a cylinder is as follows:

- robot arm should be positioned near cylinder such that the arc swept out by the proximal link intersects the cylinder and such that the plane of this arc is

roughly normal to the cylinder's central axis

- rotate Joint 1 until proximal link contacts cylinder
- rotate Joint 2 until the central link contacts cylinder
- rotate Joint 3 until distal link contacts the cylinder

This sequence is illustrated in Figure 2.17. Following this procedure will guarantee contacting the cylinder if it is within the gripper workspace. As a counter example, if the distal link moves first and the cylinder is positioned near the base of the gripper, the distal link will miss and drive to its mechanical stop. In the **PALM**, the correct sequence of link motions is accomplished with one control signal through careful choice of the mechanical coupling between the joints. The pulley and spring mechanism which implements this behavior is described in Section 3.1.

2.3.3 Passive Grasping

An important and novel aspect of the **PALM** is its passive grasping capability. Any object in contact with the mechanism applies a force which causes the links to curl around the object. This ability gives the **PALM** a high bandwidth response which allows it to come into contact rapidly with the environment. Forces applied to the **PALM** cause motion in the form of curling instead of damaging the mechanism. This behavior allows the mechanism to be somewhat compliant while exhibiting the desirable curling behavior.

The passive grasping described above is a result of cable coupling between the joints and the ratios of link lengths to pulley radii. Forces acting on the device cause it to curl until they are balanced by tendon induced moments at each joint. An important consideration is the direction and magnitude of each link's motion. A desirable behavior is curling in response to an applied force as shown in Figure 2.18. This behavior would result in the links tending to entrap the object applying the

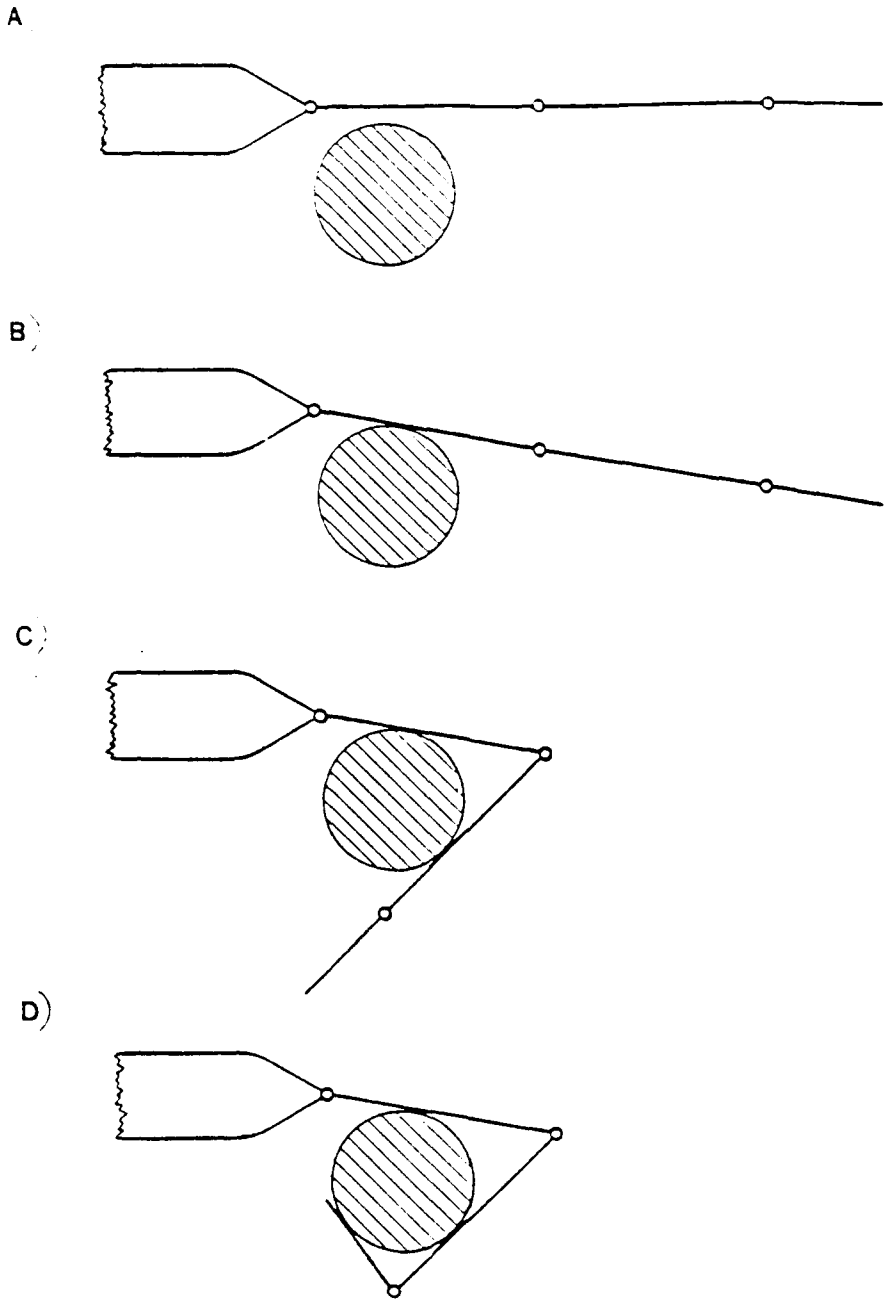

Figure 2.17: Sequence of Link Motions for Active Grasping. A) **PALM** positioned near cylinder, B) Joint 1 rotates until proximal link contacts cylinder, C) Joint 2 rotates until the central link contacts cylinder, D) Joint 3 rotates until distal link contacts the cylinder.

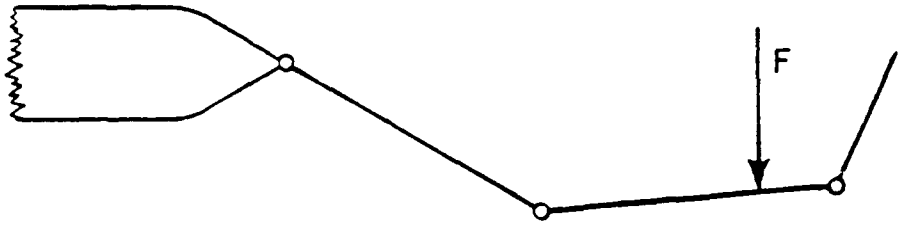

Figure 2.18: Desirable Curling Behavior

force. Undesirable responses include those shown in Figure 2.19 where the linkage buckles or bends in the wrong direction. In these instances, the mechanism is not likely to grasp the object.

This remainder of this section will show that a force applied anywhere along the links produces desirable curling (in the model of the **PALM** shown in Figure 2.15). To this end, we will first derive equations for the joint angles which result from a force applied to normal to the distal link (refer to Figure 2.20). In these equations, there are four unknowns: the cable tension, T, and the three joint angles, θ_1, θ_2, and θ_3. We solve equations and eliminate the solutions which are not physically realizable. The analysis will then be repeated for forces acting on the central and proximal links.

Forces applied anywhere along the links cause a change in actuation cable tension. The cable is modelled as a spring,

$$\Delta T = Kx \tag{2.7}$$

where T is the cable tension, K is the spring constant of the cable, and x is the cable

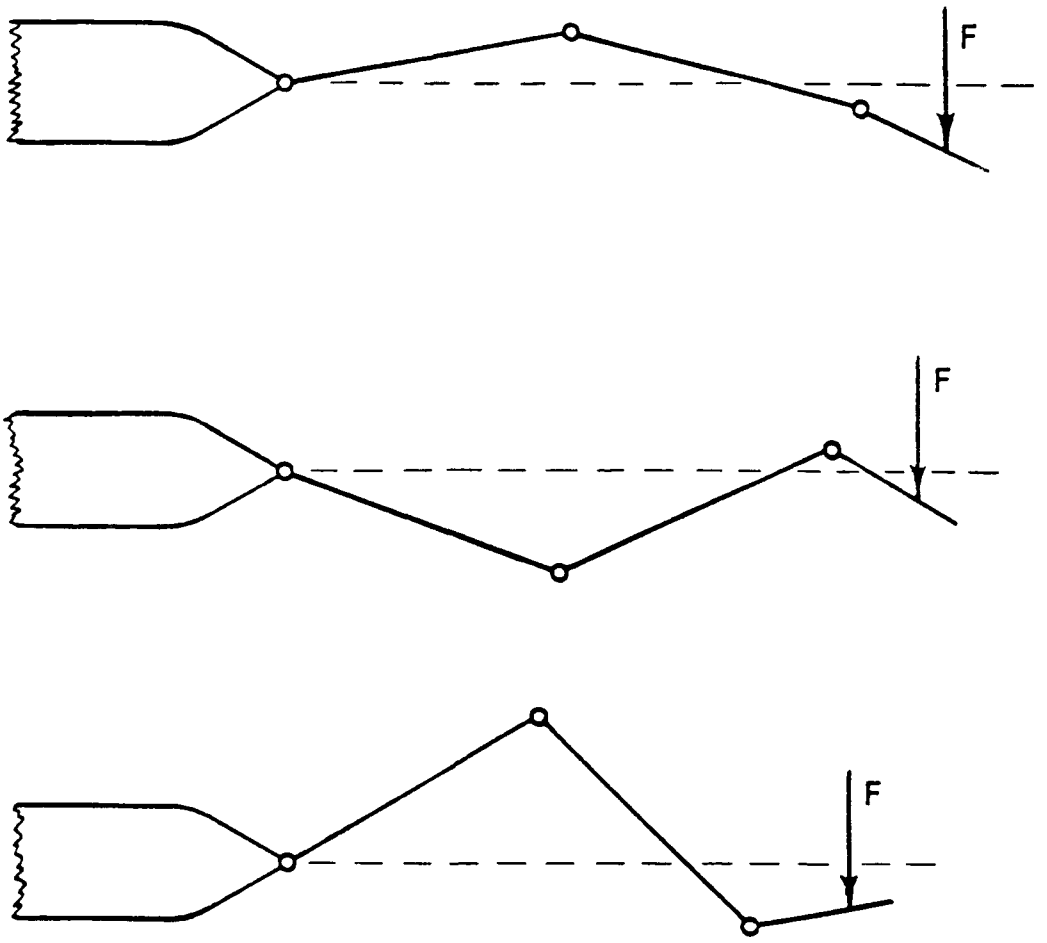

Figure 2.19: Examples of Undesirable Link Motions

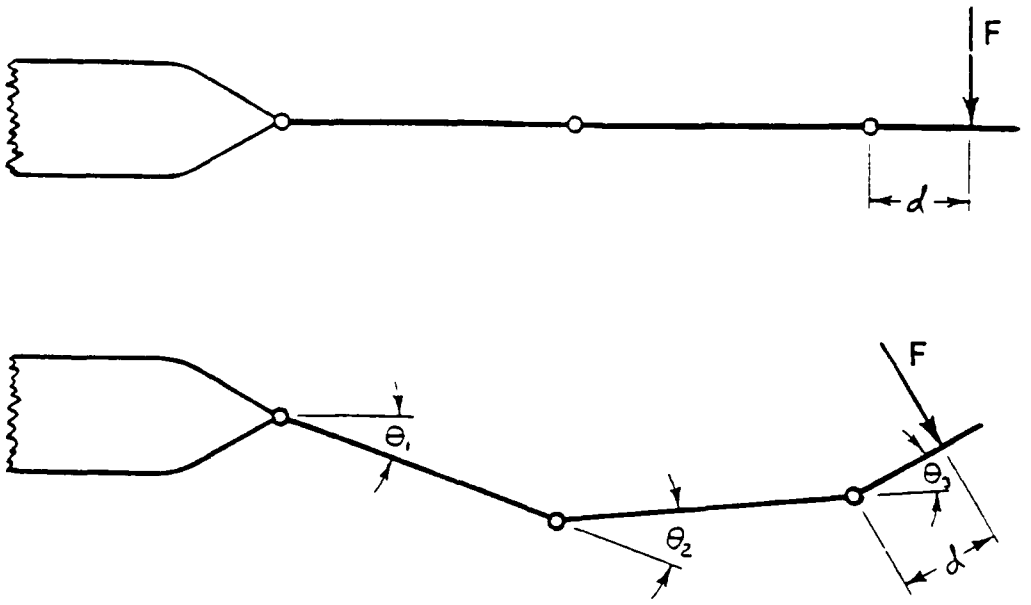

Figure 2.20: Force Acting Normal to Distal Link

displacement. For this cable path, the displacement is given by:

$$x = \sum_{i=1}^{3} r_i \theta_i \tag{2.8}$$

where r_i are pulley radii and θ_i are joint angles. If we assume that the cable is infinitely stiff, we deduce that

$$(r_1\theta_1 + r_2\theta_2 + r_3\theta_3) = 0 \tag{2.9}$$

which constrains the joint angles independent of the cable tension. Again, equation 2.9 holds for forces applied anywhere along the **PALM**.

A force applied to the distal link causes the links to move such that a new static equilibrium configuration is achieved. By equating the net torque at the each of the three joints to zero when a force acts normal to the distal link (as shown in Figure 2.20), the following equations are derived:

$$T = \frac{d \times F}{r_3} \tag{2.10}$$

$$cos(\theta_3) = \left(\frac{d}{l_2}\right)\left(\frac{r_2 - r_3}{r_3}\right) \tag{2.11}$$

$$cos(\theta_2 + \theta_3) = \left(\frac{d}{l_1}\right)\left(\frac{r_1 - r_2}{r_3}\right) \tag{2.12}$$

Springs placed between the links are ignored in these equations because their effect is negligible for all but very small applied forces. For the link and pulley ratios selected in Section 2.3.1, Equations 2.9, 2.10, 2.11 and 2.12 can be simplified to:

$$cos(\theta_3) = \frac{2d}{l_2} \tag{2.13}$$

$$cos(\theta_2 + \theta_3) = \frac{2d}{l_1} \tag{2.14}$$

$$\theta_1 = \frac{-r_2\theta_2 - r_3\theta_3}{r_1} \tag{2.15}$$

Solving these equations for a force acting on the very tip of the distal link results in a value of zero for all θ's as we would expect. For values of d greater than l_3, no equilibrium exists. To illustrate the results of Equations 2.9, 2.13, and 2.14, a simple example is provided. Suppose a force is applied halfway along the distal link, $d = \frac{1}{2}l_3$, we can solve for all three angles, $\theta_3 = \pm 60°$, $\theta_2 = \pm 120°$ or $0°$, $\theta_1 = \pm 60°$ or $\pm 12°$. The four solutions which satisfy these equations are illustrated in Figure 2.21. The first three solutions (Figure 2.21 A, B, and C) are eliminated because they are not physically realizable. In these three cases, the net motion is not in the direction of the force. Figure 2.21 D is the only realizable solution. The force on the distal link causes a clockwise torque on all the joints. Thus, the first joint experiences the most torque and starts to rotate clockwise, while the third joint which experiences the least torque rotates counterclockwise to compensate. Varying the location of the force gives results of the same form (i.e. θ_2=0 and the direction of curling is the same). These analytic results correspond to experimental results with the prototype **PALM**. In practice, however, the force does not usually remain perpendicular to

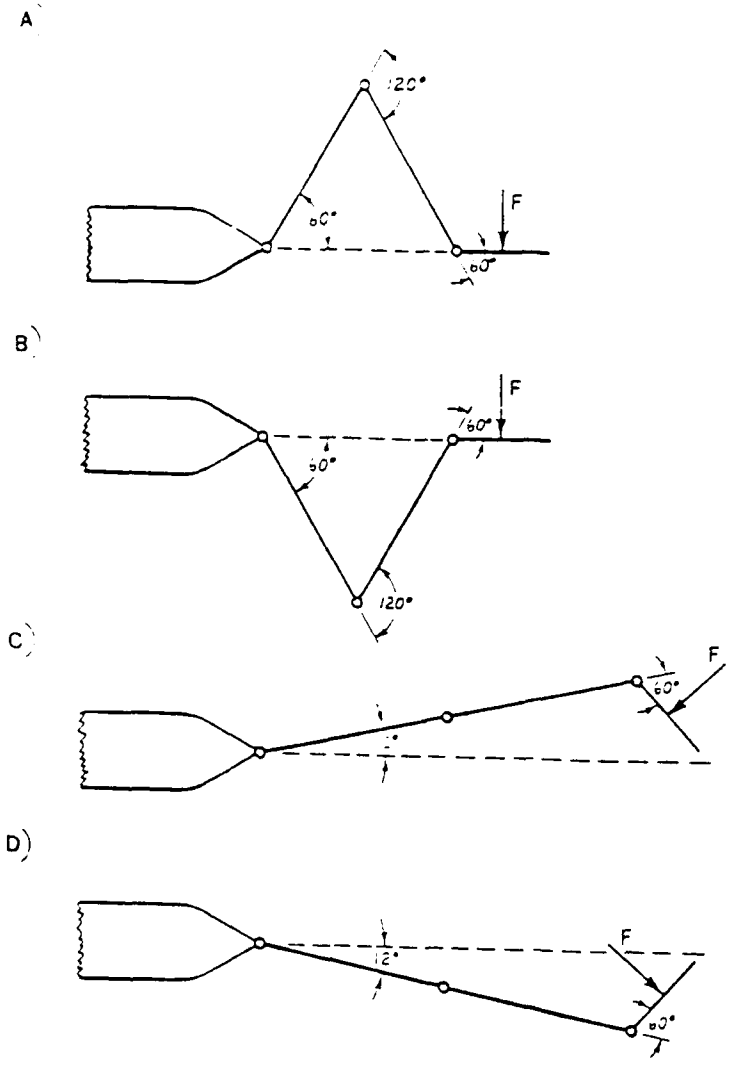

Figure 2.21: Four Solutions which Satisfy Equilibrium Equations

the distal link. This makes the equations more difficult to solve. Nevertheless, it is safe to assume that although the joint angles in the equilibrium positions would change, the direction of each links motion is the same.

The previous analysis applied only to forces acting on the distal link, but can be extended to accomodate forces on the proximal and central links as well. For example, if an object applies a force to the central link, the third link curls clockwise until it hits the object or its mechanical stop. The proximal link rotates counterclockwise, and the central rotates counterclockwise to compensate. Likewise, if an object applies a force on the proximal link, both the central and distal links ro-

tate counterclockwise until they either hit the object or their respective mechanical stops. At the same time, the proximal link rotates clockwise satisfying Equation 2.9.

Desirable passive grasping capabilities are displayed by the model presented in Figure 2.15. These results were tested on the prototype **PALM**. Photographs of the passive behavior are included in Section 4.2. The magnitude of the curling in the real system depends on the direction of the applied force, friction in the joints, tapering of the links, the stiffness of the actuation cable, and return spring force. The response was close to the predictions even though these factors were not accounted for in the model.

2.4 Quality of Grasp

A desirable criterion for a grasp is that it resists object displacements. Another measure of the grasp quality is how much external load can be applied before one or more links fail to provide positive contact. These two criterion are discussed in relation to the grasping behavior of the **PALM**.

2.4.1 Grasp Stability

As described in Section 2.1, a cylinder can be grasped in a range of configurations. Given a particular cylinder radius, we can calculate where the cylinder will tend to settle in the links. If this settling point is within a certain region, the grasp is stable. By definition, displacements from this position will cause a restoring force. Conversely, if no settling point exists, squeezing tighter on the cylinder could cause it to lose contact with one or more links.

A diagram of the force interactions between the links and the cylinder is provided in Figure 2.22. The diagram shows the centerline link lengths, l_i, the included joint angles, θ_i, and the radii of the tapered links, r_{ti}. For this analysis, the cylinder is

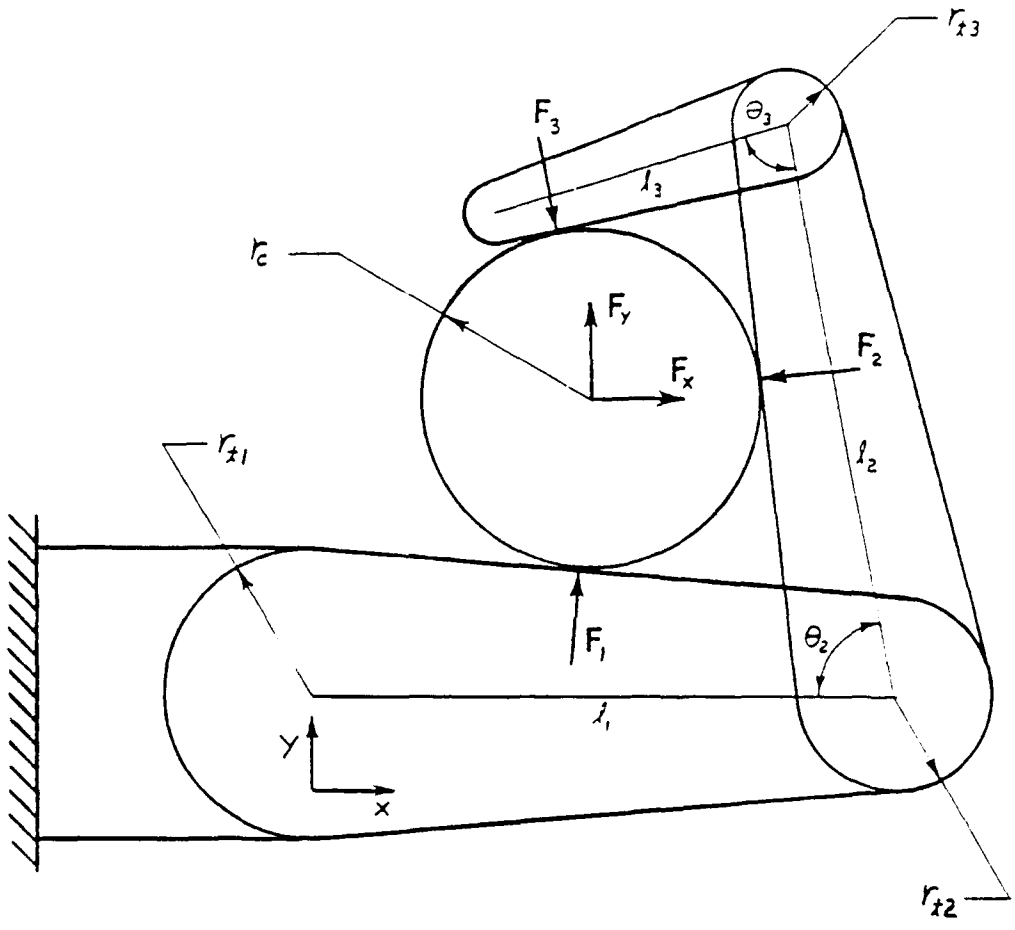

Figure 2.22: Forces on Mechanism

free to move, such that the first link is always driven to its joint limit. We assume no friction, such that all forces act along the contact normals. In this section no external load is applied to the cylinder, however, in the next section we look at the **PALM**'s behavior under external loads.

Study of Figure 2.22, leads to the following equations. The geometric constraint which must be satisfied when the three tapered links contact a cylinder is:

$$\theta_3 = 2 \times tan^{-1}\left[\frac{(r_{t3}+r)tan\left(\frac{\theta_2}{2}\right)}{\sqrt{l_2^2-(r_{t2}-r_{t3})^2 tan\left(\frac{\theta_2}{2}\right)}-(r+r_t 2)}\right] \tag{2.16}$$

The equilibrium equation for the forces acting on the cylinder can be expressed as

a function of the joint angles:

$$\alpha = sin^{-1}\left(\frac{r_{t2} - r_{t3}}{l_2}\right) \tag{2.17}$$

$\sum F_x = 0 \Rightarrow$

$$-f_3 sin\left[\theta_2 + \theta_3 + \alpha\right] - f_2 sin\left[\theta_2 + \alpha\right] = f_{bx} \tag{2.18}$$

$\sum F_y = 0 \Rightarrow$

$$f_3 cos\left(\theta_2 + \theta_3 + \alpha\right) + f_2 cos\left(\theta_2 + \alpha\right) - f_1 cos\alpha = f_{by} \tag{2.19}$$

where the symbols f_2, f_3, f_{bx}, and f_{by} are percentages of the cable tension, $\frac{F}{T}$. Since, for this analysis, no external loads are applied to the cylinder, f_{bx} and f_{by} are zero. These nonlinear equations were solved numerically for the range of cylinders which can be held in form closure to obtain the graph shown in Figure 2.23.

To experimentally validate these results, it was noted that the stable grasp can be found by modeling the actuation cable as a spring and determining the grasp configuration at which this spring stores the least energy. Thus, the results obtained above were recalculated by minimizing the cable length with respect to the settling point. Tapers were included in the model to generate data for the first prototype **PALM**. Thus, by attaching a spring in series with the cable and running the **PALM** through a range of configurations, the minimum force (corresponding to the minimum spring deflection) was measured by a force gauge. Figure 2.24 shows the two sets of collected data and the theoretical curve. No data was collected to verify the increasing portion of the theoretical curve because the links of the first prototype **PALM** interfered with each other in these grasp configurations. The links in later versions are designed not to interfere. Inaccuracies in the readings result from the force measurements being insensitive to small movements about the minimum energy point.

From this analysis, we can see that the gripper tends to pull cylinders into stable grasps. This action increases the **PALM**'s workspace considerably. The mechanism

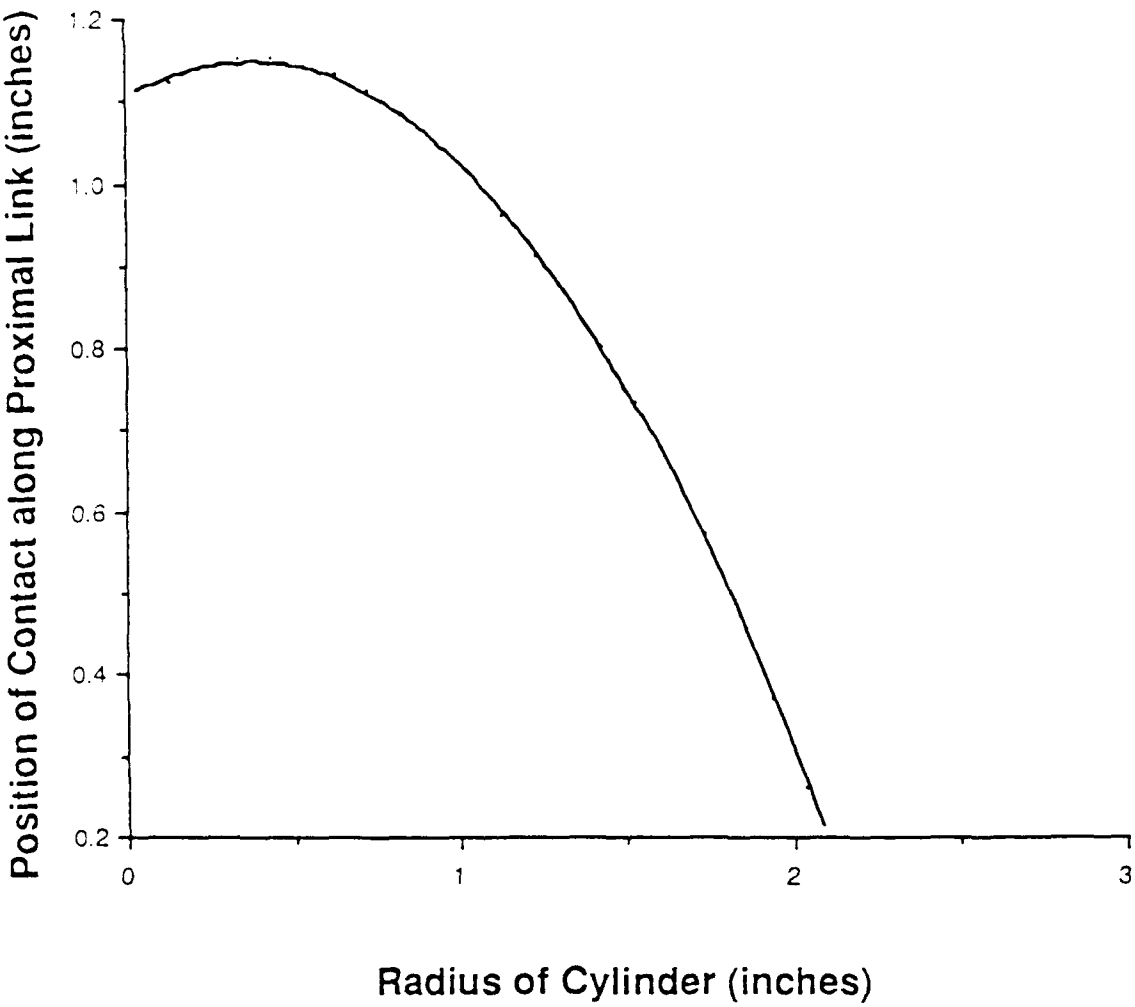

Figure 2.23: Position of Stable Grasp Configuration for a Range of Cylinders

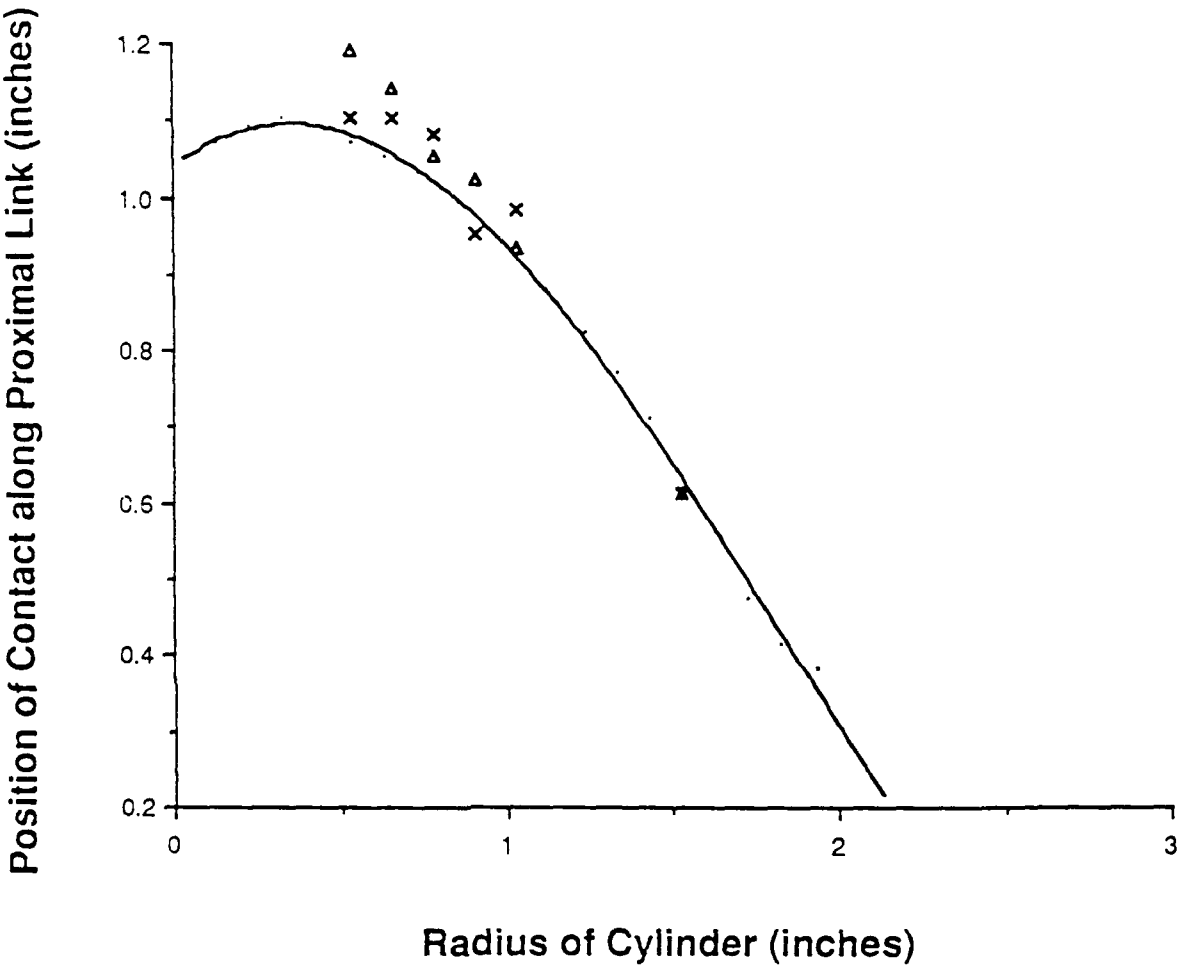

Figure 2.24: Minimum Energy Grasp Configuration

curls a "fingertip" grasp inward until contact occurs on all three links. Then, the links squeeze against the cylinder until it moves into a stable, form closure grasp.

2.4.2 Load Capacity

An external load that is applied to the cylinder causes the equilibrium equations to change (i.e. f_{bx} and f_{by} in Equations 2.18 and 2.19 become nonzero). A new equilibrium point can sometimes be found. The load capacity is the maximum externally applied force for which a physically realizable equilibrium point can be found. The modes of failure that can occur are:

1. Lose contact with proximal link: F_1 goes to zero.
2. Lose contact with central link: F_2 goes to zero.
3. Proximal link moves: the force on proximal link overcomes the torque exerted by Joint 1.
4. Cylinder slips off distal link.

These failure modes are illustrated in Figure 2.25. Friction contact between the cylinder and the links will help avoid these conditions by opposing the motion of the cylinder. The load capacity is a function of the loading direction. Intuitively, the smallest capacity should be felt when the load acts on the last and weakest link. Figure 2.26 shows in detail the theoretical maximum force as a function of loading direction for selected cylinder radii. These plots scale with the cable tension. For each radius, four lines enclose an area in which the cylinder will tend to settle to a new equilibrium point. These four lines define the maximum loading capacity in all directions and the numbers near them indicate which mode of failure occurs. Several interesting features in these plots should be noted. Failure conditions 1 and 3 form vertical lines. This indicates that the x component of the force is constant. In other words, there is a threshold force in the x direction after which the grasp is

not stable. Another interesting feature is the large peak in maximum force in the third quadrant. This occurs because most of the external load is carried by the first joint which supplies the most torque.

If a more evenly distributed loading capacity is required, the above analysis can be used to vary the physical dimensions of the **PALM**, thereby shifting the curves (shown in Figure 2.26). However, this would affect the passive grasping capabilities described previously. For example, the gripper may not remain in static equilibrium when a force is applied to the tip. Alternatively, the information from these curves could be used by an intelligent robot system to select the best grasp orientation in anticipation of greatest loads, or apply force in the directions where the mechanical advantage is greatest.

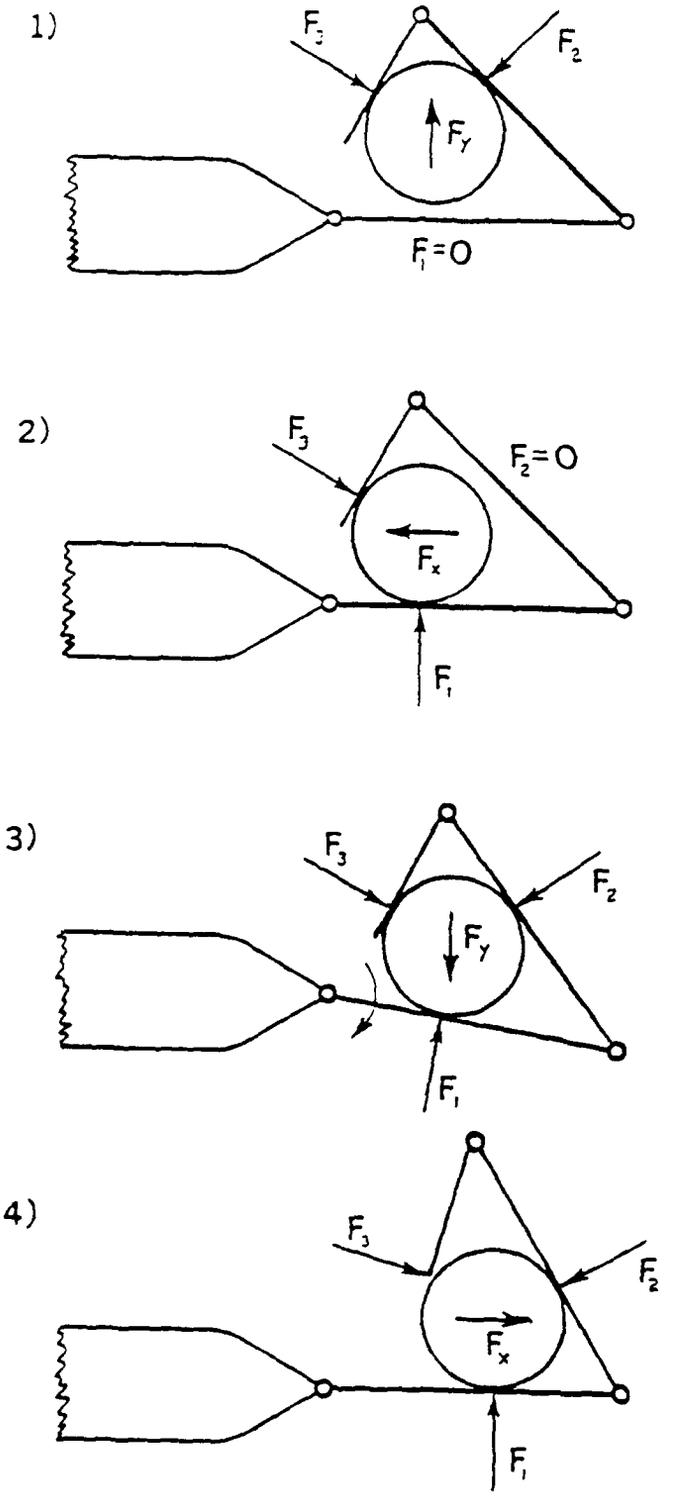

Figure 2.25: Modes of Grasp Failure.

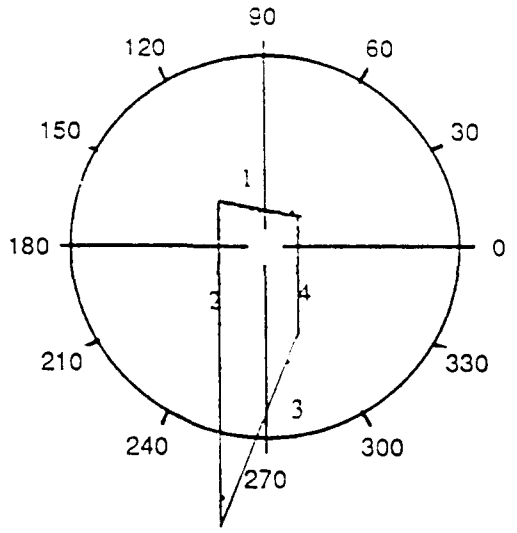

A) Radius = 0.25"

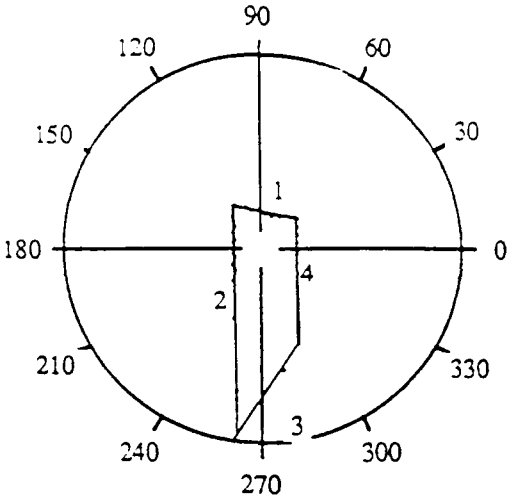

B) Radius = 0.5"

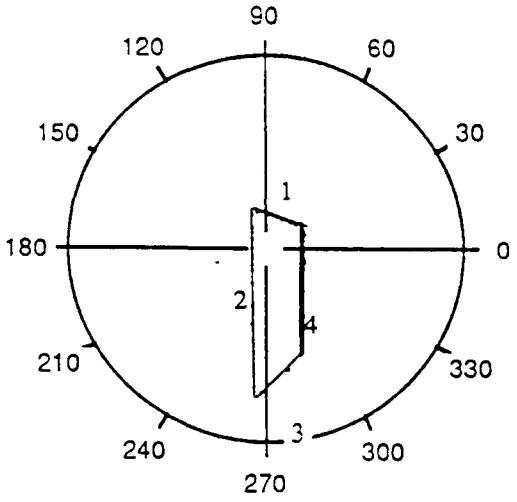

C) Radius = 0.75"

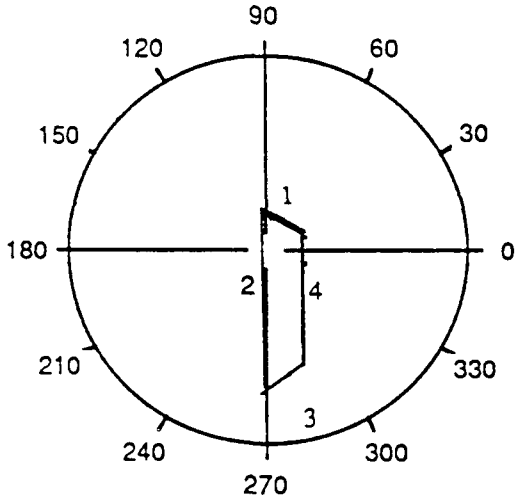

D) Radius = 1.0"

Figure 2.26: Load Capacity. The cable tension is represented by the outer circle. Numbers around the circle indicate the direction of the external load, applied through the cylinder's center. The magnitude of a vector from the origin to any point on the graph gives the loading capacity in the direction of the vector.

Chapter 3

Mechanical Design

3.1 Gripper Design

A prototype version of a **PALM** was built to demonstrate its unique capabilities. The particular mechanical design used to achieve this behavior is described in this section. This **PALM** is a one actuated degree-of-freedom device consisting of three links and three joints as illustrated in Figure 3.1. A drive motor is located at the base of the finger, near the robot's wrist. Two steel cables (i.e. tendons) transmit the actuation forces via pulleys to the joints allowing finger flexing and extension. Springs placed between the links eliminate kinematic indeterminacies in the joint positions, and consequently dictate the curling characteristics.

Keeping the weight of a robot end-effector low is a very important consideration because the moment arm from it to the robot joints is large. Having only one actuated degree of freedom results in fewer motors, and consequently a lighter end-effector. Cable drive allows the weight of the actuator to be concentrated towards the base of the finger. The links have also been tapered with a high aspect ratio, further reducing the loading on the arm. Various components of the design are discussed below.

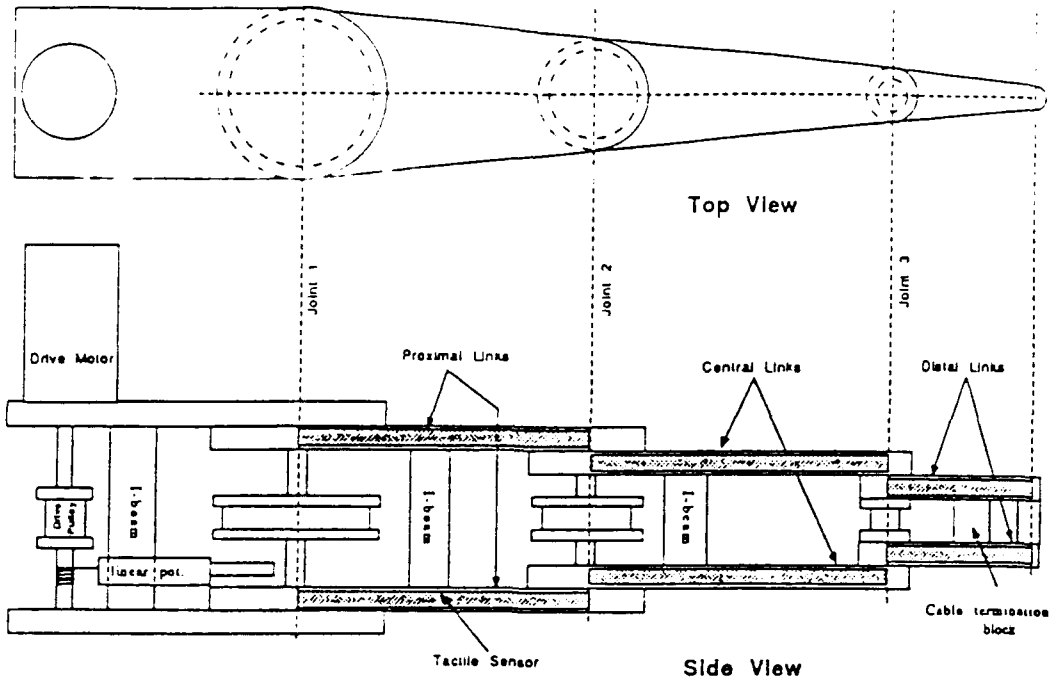

Figure 3.1: Drawing of PALM

3.1.1 Links

The link lengths were chosen to facilitate grasping a three inch diameter cylinder, which is approximately the diameter of current space trusses. Using the link ratios selected in Section 2.1 the centerline lengths of the proximal, central, and distal links are 4 inches, 4 inches, and 2 inches, respectively. Even though a greater range of cylinders can be grasped with a longer gripper, the tradeoff is an increased mass on the robot and added unwieldliness.

Each link has two sides (shown in the side view in Figure 3.1). These sides are made of 0.25" inch thick Delrin. The 0.25" gripping surface provides a large area of contact between the gripper and the cylinder. Tactile sensors are positioned along this surface (the design of these sensors is dicussed in Section 3.2). Starting from the distal link, the links fold inside each other. The distance between the two sides of each link range from $1\frac{3}{4}$" to $\frac{5}{8}$". These large distances between the gripping edges make it possible to apply moments to a long truss.

The sides of each link are attached to each other in two places. This makes the mechanism more sturdy, and resists skewing caused by a force acting on just one

side of a link. The two sides of each link are connected by the I-beam shown in Figure 3.1, and the outermost sides of each joint are rigidly attached to each other through the joint shafts.

3.1.2 Drive Mechanism

The drive mechanism consists of a motor, drive pulley, and linear potentiometer. The motor is a DC brush type with a 60:1 gearhead (Escap L28 219). Attached directly to the gearhead shaft is a 0.5 inch diameter drive pulley. This combination of motor and drive pulley was selected such that the **PALM** can apply a 5 lb force with the tip of the last joint. A linear potentiometer is coupled to the drive pulley via a small diameter steel cable. Position information from this potentiometer is used to center the drive pulley and the actuation cables. Springs resolve the remaining indeterminacies in link positions as discussed later in this section.

3.1.3 Cabling

Two steel cables which actuate the **PALM** are routed as illustrated in Figure 3.2. Both cables are wrapped around the same pulley in opposing directions. These cables are nylon covered, 0.031 diameter stranded steel manufactured by SAVA Industries. The pullies on the first and second joints are idler pulleys. Thus, when the proximal or central links are restrained the actuation force is still transmitted to the succeeding joints. Symmetry in the cabling allows the gripper to be bidirectional.

The cables are tensioned by threaded cable crimps attached to the distal link. To keep both cables taut under maximal loading, they should be pretensioned to half the final cable tension which is about 50 lbs with the current drive system. This pretensioning would result in the one cable just beginning to go slack when the other is fully loaded. This is not done in the current prototype because it causes to much friction in the joints. The joint bearings currently consist of a Delrin link

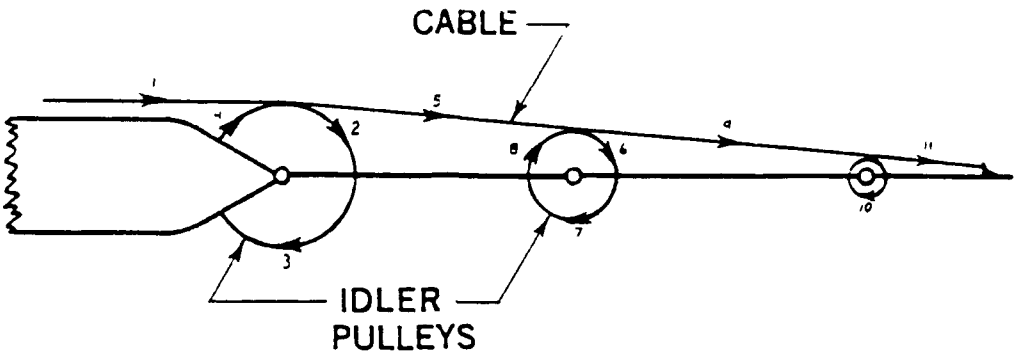

Figure 3.2: Cable Path

rotating on a steel shaft. A solution to this problem would be to place ball bearings in the joints.

3.1.4 Springs

Springs placed between the joints serve three functions: return links to center position, dictate curling order, and compensate for gravity. These functions and how they effect the choice of springs are discussed below. Then, two spring mechanisms and the tradeoffs between the two are presented.

Firstly, the springs apply a restoring torque which returns the links to the center position. At this position, the springs store minimum energy. The ratio of spring constants is not important for this function. The torque that the spring supplies to the joint could be constant if its magnitude is enough to overcome friction when the joint is rotated off-center.

Secondly, the springs eliminate indeterminacies in the position of the links when no external forces are applied. These springs are selected to cause the links to move in the following order: proximal, central, then distal. To have a particular joint rotate, the torque applied by the cables must overcome the restoring torque

supplied by the spring. To dictate the proper sequence of link motions, this rotation of a particular joint must start at a higher cable tension than in the preceding joints. The springs used in the prototype supply a constant force insuring that one joint moves all the way to its joint limit before the next one starts to rotate. However, if it is desired to make the links curl with a particular ratio of joint angles, the spring constants of linear extension springs can be chosen to cause this behavior.

Thirdly, springs compensate for the fingers weight when fully extended. To avoid sagging it was desired that the springs provide a step function in torque about the joints. The magnitude of the torque step must be enough to compensate for the gravity load acting on each joint. However, it is difficult to satisfy this condition and the second criterion that the proximal link move first. It is necessary to notice that if the cable length is constant at least two links must move at once. Therefore, if the outer links are overcompensated, less of a step can be applied to the base links while sagging is still avoided.

Two mechanisms that provide a step function in torque are shown in Figure 3.3. The first, 3.3 A, is used in the prototype **PALM**. This mechanism uses a constant force extension spring coupled to a pulley via two cables. Constant force springs are used in this design to avoid unnessesary energy storage and consequent loss of grip force. The torque on the joint is selected by varying the pulley diameter. As the pulley starts to turn, the force is transfered instantly from both cables into one, resulting in a step increase in torque. This step is illustrated in Figure 3.4 A. One problem with the design is that one cable always becomes slack when the link turns. The length of the slack portion is reduced by attaching the cables at the point where they lie tangent to the pulley. The guide hole helps keep the cable constrained.

The second mechanism, shown in 3.3 B, uses a torsional spring preloaded against pegs to create a step function. The restoring torque applied to the joint by this mechanism is illustrated in Figure 3.4 B. The spring is situated such that its axis is aligned with the joint axis. When the link starts to turn, one leg of the spring is

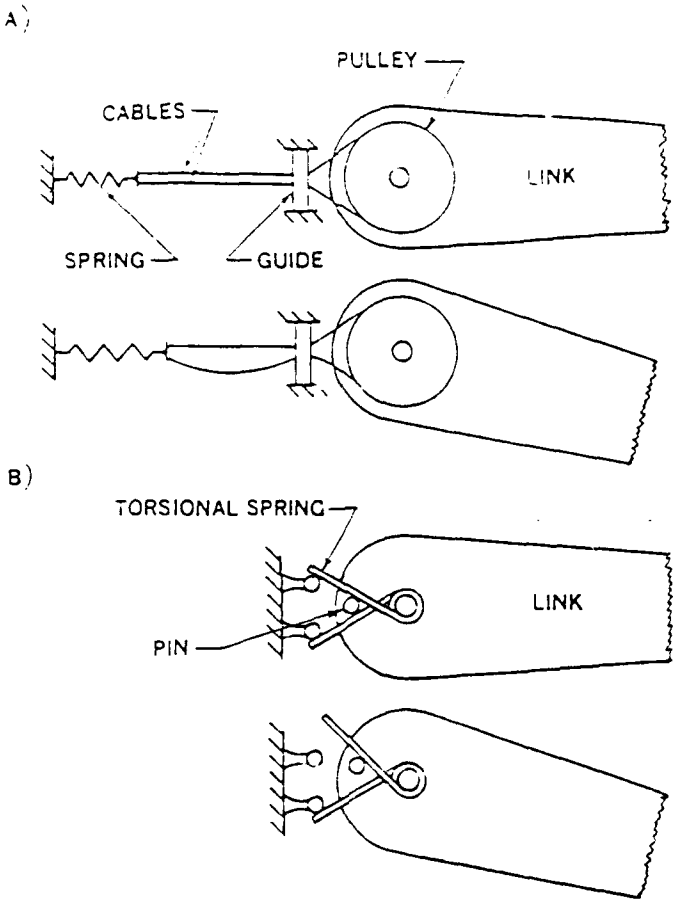

Figure 3.3: Spring Mechanisms. A) uses a constant force extension spring coupled to the joint through a pulley and cabling, B) uses a torsional spring on the joint axis.

fixed and the other moves with the link. Likewise, when the link turns in the other direction the same spring hits against the other stop providing the step in torque. One problem with this design is that the position of the pegs must be precisely aligned or adjustable to achieve accurate centering of the link. Also, unlike the previous design the torque constants cannot be selected arbitrarily because torsional springs typically can only be found in certain sizes. Despite these disadvantages, a third smaller prototype PALM is currently being fabricated using this design. Space limitations prohibited the use of constant force springs in this version. Furthermore, the torsion springs can be totally encased in the links making a very clean design.

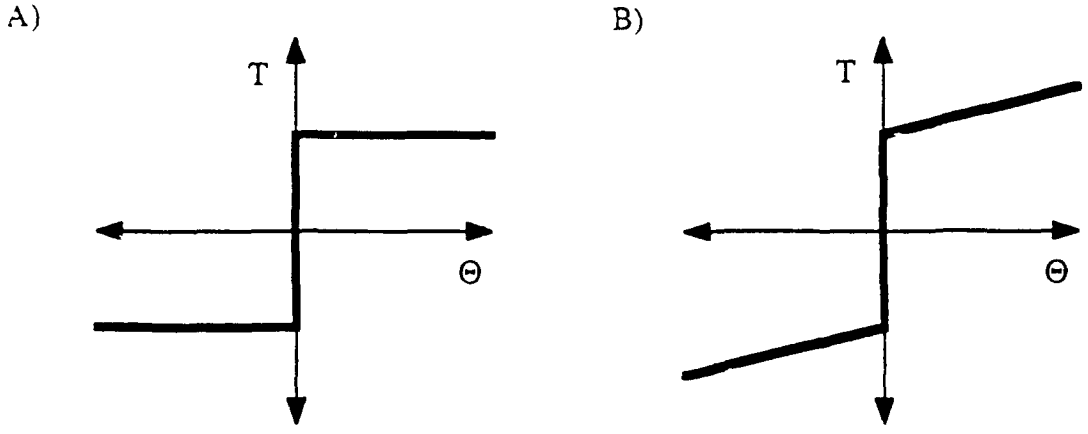

Figure 3.4: Restoring Torque Versus Displacement of Joint. A) Step function created by constant force spring, B) Step plus ramp function created by torsion spring

3.2 Tactile Sensors

Sensory information from a robot end-effector should be used to guide the robot system and confirm acquisition. In this section, the sensor design criteria for this application are discussed. Alternate designs that were considered are presented, and their weaknesses are pointed out. Then, the tactile sensor which was designed for this application is described.

3.2.1 Sensory Needs

The sensory needs of a system should be examined carefully in order to select the right type of sensing. In this application, a sensor that gives the position of a contact along one axis would fulfill all the needs. First, information from the sensor can be used to align the gripper and cylinder. Misalignments can occur about the roll and yaw axes of each link. Misalignment about the roll axis means that only one side of a link makes contact, and misalignment about the yaw axis implies that the two sides

of each link make contact at different locations. Secondly, tactile information is used to determine if the grasp was successful (i.e. one contact on each link). If the grasp is unsuccessful, the information could be used to determine the mode of failure. For example, if only the central and distal links show contact, the control system should advance the arm forward and try the grasp again. Thirdly, determining a grasped object's position and orientation in the **PALM** is also critical because the contact locations for a given cylinder are not unique. Thus, sensors which can distinguish the position at which contact occurs are needed. As a further consideration, it is advantageous to minimize the number of wires running to each sensor because of the rotation of the joints and limited space.

3.2.2 Alternate Approaches

Several ideas for position sensors were considered for this application. One potential candidate was conductive-ink tactile sensors [5]. Pressure on these sensors cause the conductive ink to deform and its resistive properties to change. Thus, through a linear array of pixels, both force and position can be distinguished. However, these sensors were rejected for this application because they require too many wires to obtain the necessary spatial resolution. Microswitches embedded in the joints were another option. One scheme to reduce the wiring, would be to multiplex the resistors as shown schematically in Figure 3.5[4]. Thus, the voltage drop could be used to indicate which microswitches were activated. This idea was not pursued due to packaging problems and the number of moving parts involved. A third option was a beam simply supported on both ends by load cells (shown in Figure 3.6). The ratio of the force readings from these two cells can be used to determine the position of the contact. However, commercially available miniture load cells were too expensive for this application. One other idea worth mentioning is a simply supported beam with two strain gauges attached as shown in Figure 3.7. When a contact occurs between the gauges, the gauge readings can be used to locate the point of contact. However,

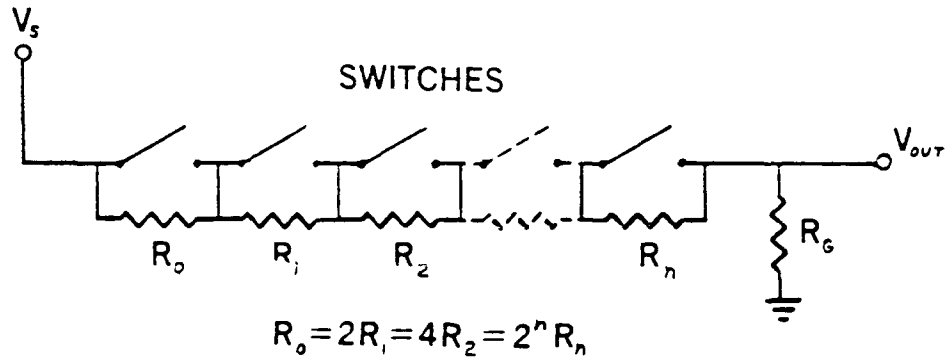

Figure 3.5: Multiplexed Resistor Network

if the contact doesn't occur between the gages, the location is indeterminate. Thus, it would be necessary to place the strain gauges by the ends of the beam where the stresses are lowest. This would result in poor position resolution, and hence the idea was not pursued.

3.2.3 Sensor Description

The sensors which were developed and incorporated into the prototype **PALM** are linear position sensors. These sensors consist of a sandwich of three components: a sensing plate, conductive material, and an insulator. An electro/mechanical schematic is provided in Figure 3.8. The components are arranged such that the sensing plate is embedded in a groove on the surface of each link. The conductive material straddles the groove and is about .001" above the sensing plate. An insulator covers the conductive material electrically isolating it from the external environment. A force on the link surface will cause the conductive material to deform into the groove and make electrical contact with the sensing plate.

An electrical equivalent of the system is given in Figure 3.9. In this circuit,

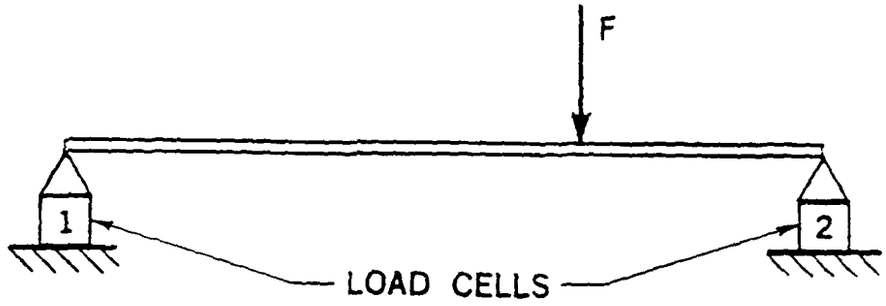

Figure 3.6: Load Cell Tactile Sensor

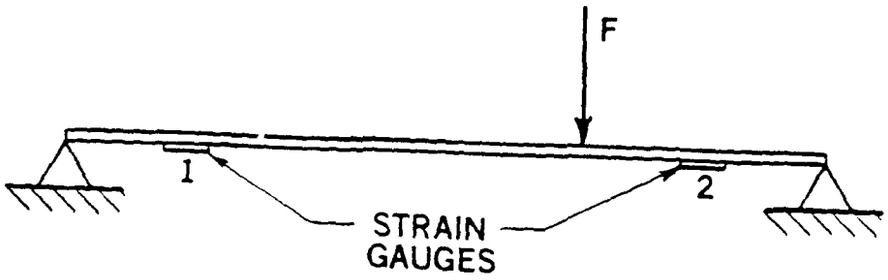

Figure 3.7: Strain Gauge Tactile Sensor

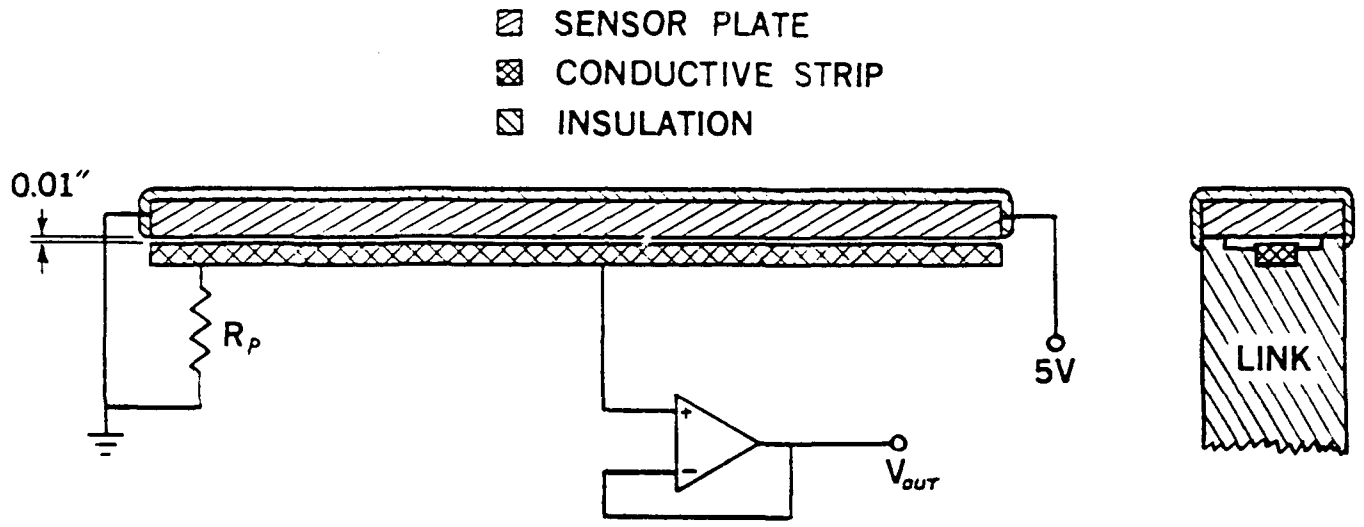

Figure 3.8: Electro-mechanical Schematic of Tactile Sensors

$\mathbf{R_p}$ is a pull-down resistor, $\mathbf{R_c}$ is the resistance at the contact between the conductive material and the sensing plate, and $\mathbf{V_{out}}$ is the voltage that is read from the sensor. The conductive material is modelled as a potentiometer. Because of the high impedance of the operational amplifier and pull-down resistor, only a negligible amount of current flows through $\mathbf{R_c}$. Therefore, the position of contact is proportional to $\mathbf{V_{out}}$.

$$x = \frac{V_{out} \times L_f}{V_s} \tag{3.1}$$

where L_f is the length and V_s is the potential across the conductive material. Multiple contacts cannot be distinguished. In this case, the reading will look like a single point contact acting between the contacts However, the specific location is now a function of the ratio of contact resistances, $\mathbf{R_c}$, because the current flowing through $\mathbf{R_c}$ is no longer negligible.

Experimentation with alternate materials led to the selection of ones which work well for this application. Gold plated nickel is used as a sensing plate because it makes good electrical contact and it doesn't oxidize. The first sensors were made with brass sensing plates whose performance degraded over time because of oxida-

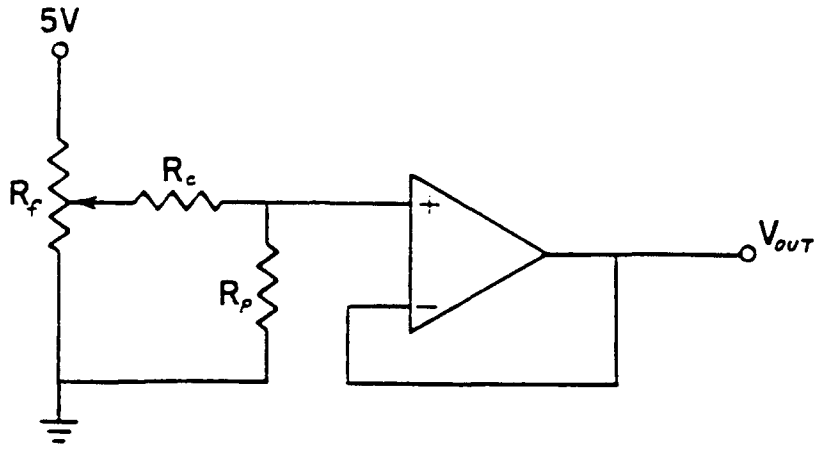

Figure 3.9: Electrical Schematic of Tactile Sensor

tion. Conductive foam was selected because of its elasticity. Preliminary experimentation with conductive rubber also showed promising results. The insulator is a coat of solethane, a flexible adhesive.

Results from a prototype version of the sensor show linear behavior as illustrated in Figure 3.10. An approximate spatial resolution was obtained by taking data from several trials for eight different positions. The spatial resolution is the maximum error in position as labelled in (Figure 3.10). A dimensioned drawing of the sensors for which this characterization was performed is provided in Appendix A.

These position tactile sensors were designed specifically to be incorporated into the links of the **PALM**. However, they can be used for any application where low-resolution tactile sensing is needed. Their compactness and low number of wires make them ideal for robotics. For example, a robot could have strips embedded in its links running lengthwise. The information from these sensors would determine if the robot was touching something and the approximate location of contact.

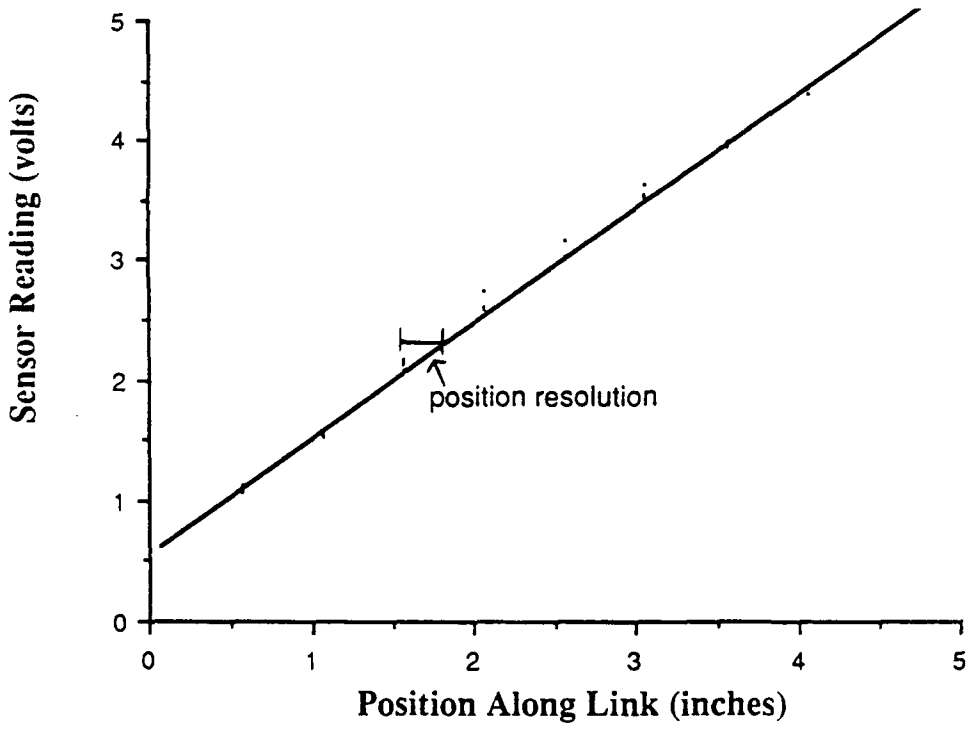

Figure 3.10: Sensor Characteristic Curve

Chapter 4

Operation and Evaluation

4.1 Operational Modes

The **PALM** has three basic modes of operation: reflexive, active gripping, and returning to center. In the reflexive mode, the **PALM** servos the motor on center until the tactile sensors are activated by a contact. The contact causes the controller to enter active gripping mode and curl in the direction of contact. When commanded to release, the **PALM** uses position information to servo back to center. It is important to remember that the actuator only centers the cables while the springs placed in the joints ensure that the links are centered. A block diagram of the control system and electronic schematics are presented in Appendix B.

4.1.1 Reflexive Mode

In reflexive mode, the tactile sensors are scanned while the **PALM** is position servoing on center. When the **PALM** comes into contact with an object, it complies and curls passively about the point of contact. As soon as any tactile sensor is activated, the control system switches to the active gripping mode. However, if the tactile readings are not within given constraints, the controller should transmit

the position information to the robot control system so it can take the appropriate action, by either moving the gripper forward or rotating to correct misalignments. For example, when gripping cylinders there are two degrees of freedom (roll and yaw axis) about which a cylinder can be misaligned. The tactile sensing information is rich enough to have the robot comply about the appropriate axes.

4.1.2 Active Grasping Mode

To actively grasp an object, the links must curl around it and squeeze. To accomplish this, the motor which drives the actuation cables employs hardware current control. Current control is used because we wish to control the torque in the drive pulley when grasping (the current control circuitry is included in Appendix B). As described previously, actuation causes the links to curl until they contact the object or reach their joint limits in the following order: proximal, central then distal. Tactile sensor readings are scanned during the grasp. This is a very important feature for grasp verification. When all three links come into contact, the grasp is considered complete and the robot can perform its next maneuver. Also, if the links don't all contact, the tactile information can be used to decide on the appropriate recovery action, for example, an ungrasp followed by a second attempt at grasping.

4.1.3 Release Mode

The PALM has two options in ungrasping an object. It can perform a "soft release" in which the current is simply turned off. Or, as is the case most often, the **PALM** will position servo back to the center position. In the current implementation, the position servo is a PID controller. The PALM is a highly nonlinear system, and no attempt was made to model it. The sample rate of the position servo is 200 Hz (100 Hz when scanning the sensors). Control gains were picked to achieve (as closely as possible) desired characteristics such as fast response, no overshoot, no steady-state

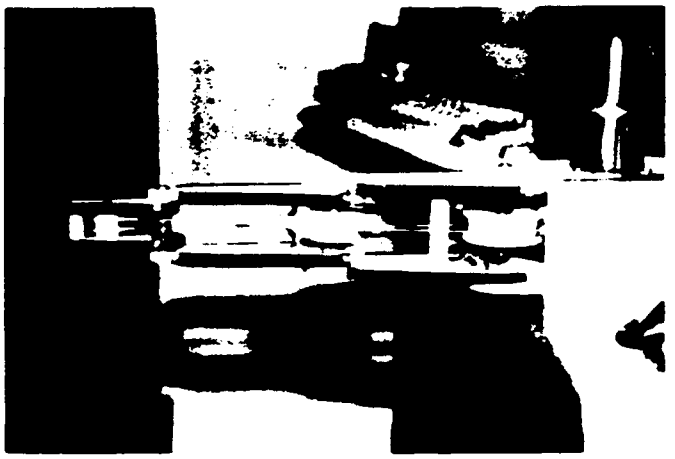

Figure 4.1: Prototype **PALM**

error. The proportional gain is turned up high with a large derivative term to damp the overshoot. Integral feedback is added mainly to bring the gripper to the home position when acting against gravity. A saturation non-linear element is added to the integral term to avoid wind-up.

4.2 Evaluation

In this section, important features of the **PALM** are discussed in relation to experience in the lab. Figure 4.1 shows a photograph of the actuated prototype **PALM**. The base link is clamped rigidly to the egde of a table for these tests. The black strips on the edges of the links are the tactile sensors. This version is 10" long from the first joint to the tip of the distal link.

The key purpose of this project was to design an end-effector which works well on a simple class of objects. The prototype **PALM** is shown in Figure 4.2 grasping a variety of diameter cylinders. As you can see, all these cylinders can be grasped adequately. However, for the smaller diameter cylinder especially, the pri-

mary workspace is limited. To improve the workspace in constructing a new version, the ratio of link would be changed such that the distal link is proportionally a bit larger. The positive aspects of current lengths are that the mechanism does not typically hit into itself with the tip of the last link. On the other hand the most common mode of failure during grasping is that the distal link doesn't reach the cylinder. A larger distal link increases the primary workspace for small diameter cylinders.

The diameter of cylinders which can be grasped depends on whether the cylinder is in the primary or secondary workspace. Figure 4.3 shows one secondary workspace grasp. In a zero- gravity situation, this cylinder would be brought into a form closure grasp. The application of this to space truss acquisition is important. It is resonable to assume that space trusses are not free floating until they have been grasped by the **PALM**. At this point they are released and the gripper pulls them into a tighter grasp.

Figure 4.4 shows the **PALM** passively curling about cylinders with no actuation. In these photographs, the cylinders are applying a force to the links. The gross behavior (i.e. the direction of curling of each link) corresponds to the analysis in Section 2.3. However, due to friction and the springs in the joints, the exact angles cannot be calculated with great accuracy. Note that in Figure 4.4 A, the second joint remains stationary as predicted by the analysis in Section 2.2. In Figure 4.4 C, the distal link does not rotate. If the mechanical stop on the first joint is removed all the links rotate to contact the cylinder. The joint stop exists to insure that the mechanism does not pull object against its own base. The joint stop can be moved such that the range of joint motion increases insuring better passive grasping.

The quickness of the prototypes passive response can be demonstrated by placing it in reflexive mode, and slamming a cylinder against the links. As expected, the mechanism passively curls about the object. Upon aquiring the tactile information (100 Hz) the arm actively drives all the links into contact. One problem with the

Figure 4.2: Prototype **PALM** Grasping a Range of Cylinders

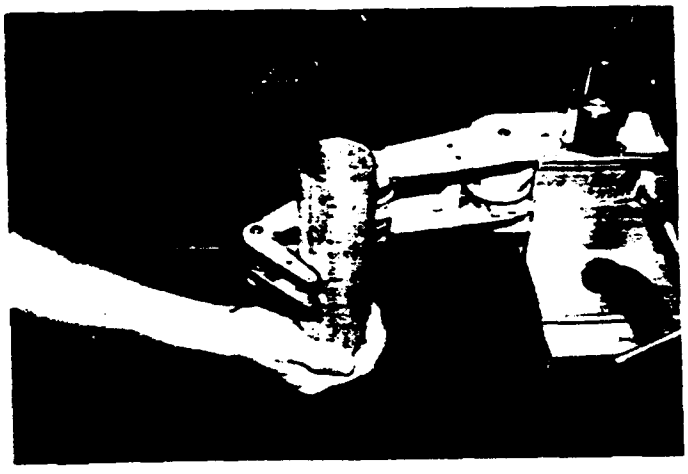

Figure 4.3: Secondary Workspace Grasp

design is that a contact at the very tip of the distal link produces no motion (see Figure 4.5). If this contact occurs at high speed the mechanism could be damaged. Realizing this, in the most recent prototype of the **PALM** the pulley ratios are selected such that a force anywhere along any link produces desirable curling. This is done by making the focal point (the point where a force can be applied such that the gripper remains in equilibrium) past the tip of the distal link.

Figure 4.4: Prototype **PALM** Displaying Passive Grasping. A) Contact on distal link, B) Contact on central link, C) Contact on proximal link.

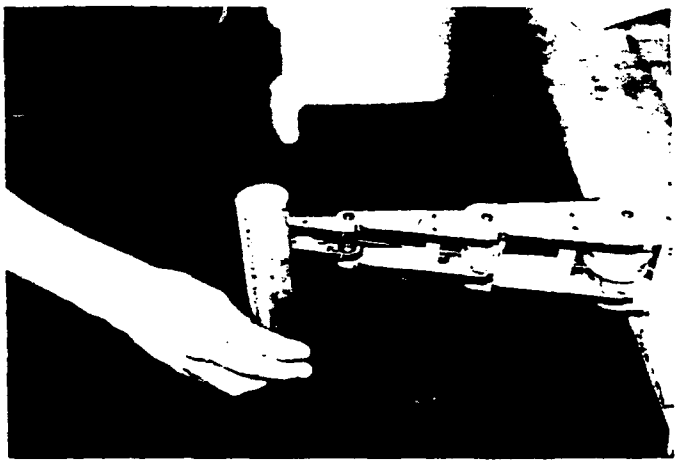

Figure 4.5: Prototype **PALM** in Equilibrium

Chapter 5

Conclusions

5.1 What Has Been Done

A mechanism was designed for grasping a specific class of objects, cylindrical in this case. Early in the design process, it was decided that compliant charateristics were needed to be able to collide with the environent at high speed. Analysis was performed to determine the relevant kinematics, the workspace, the grasping behavior, and the quality of the grasp. A prototype was constructed to evaluate the design and analysis.

This was a first prototype of a new type of gripper which combines passive and active grasping capabilities. The mechanism currently works well as a palm which can grab cylinders rapidly from either side. Natural "grabbiness" and high bandwidth response to forces makes this device a good candidate for a gripper that will come into contact with objects rapidly.

5.2 Future Directions

An end-effector such as the **PALM** should be designed to be very strong so it can not only grab but also pick up heavy objects. This project concentrated on a mechanism

to improve grasping. The load capacity was analyzed but no attempt was made to increase it. An improvement to the design would be to increase the strength while maintaining the same desirable grasping characteristics. The structure is sturdy enough to take more load. However, in the present design, the cables are loaded to their rated tension when grasping at full power. One way to make the device stronger is to increase the motor power and use thicker cables. However, thick cables fatigue rapidly and exhibit greater friction when wrapped around small radius pulleys. Therefore, increasing the effective thickness of the cable by running several smaller ones in parallel is a good option. Another possibility to improve the strength is to employ a block and tackle mechanism. This would act similarly to another gear stage, increasing the force while decreasing the speed.

Protecting the moving parts of the mechanism would also be a valuble improvement. Before operating the device in a real environment, it would probably be necessary to enclose the cable paths and the pulleys. This is a non-trivial design task with the current configuration of the **PALM** because a protective covering would prevent the links from folding inside each other.

I believe that the newest prototype which incorporates torsional springs in the joints is more robust than the design evaluated in Section 4.2. This design has the additional advantage of enclosing the springs from the environment. The mechanism which provides the step function works well to prevent the links from sagging. However, it is very tediously to align the pegs. If the spring legs deform even slightly, it will need realigning. An adjustable alignment mechanism could be designed.

The use of two or more of these devices acting in opposition would create an end-effector with unique characteristics. The advantages of the **PALM** design would be maintained and some of the problems resolved. With more gripping surfaces, the device would be able to grasp objects with more complex geometries. The gripper would be better than a parallel jaw type because it could mold itself to different shapes. It would also have advantages over current "dexterous" manipulators which

are designed to hold objects only with the fingertips. Another advantage to grabbing an object with two or more fingers is that they would constrain it to a unique configuration, and thus the object would not tend to shift in the grasp.

Bibliography

[1] J. K. Salisbury et al. Preliminary Design of a Whole-Arm Manipulation System (WAM). In *Proc. IEEE Intl. Conference on Robotics and Automation*, Philadelphia, Pennsylvania, 1988.

[2] Shigeo Hirose and Yoji Umetani. The Development of Soft Gripper for the Versatile Robot Hand. Technical report, Tokyo Institue of Technology, Tokyo, Japan, 1977.

[3] Sukhan Lee. Two-Thumbed Robot Hand. *NASA Tech Briefs*, pages 82–83, February 1989.

[4] Timothy R. Ohm. Reduced-wiring Tactile Sensor. *NASA Tech Briefs*, 1990. To be published.

[5] Robert M. Podoloff and Michael Benjamin. A Tactile Sensor for Analyzing Dental Occulsion. *Sensors*, 6(3):41–47, March 1989.

[6] Albert Rovetta and Giuseppe Casarico. On the Prehension of a Robot Mechanical Hand: Theoretical Analysis and Experimental Tests. Technical report, Institute of Mechanics of Machines, Polytechnique of Milan, Italy, 1980.

[7] J. K. Salisbury. *Kinematic and Force Analysis of Articulated Hands.* PhD thesis, Department of Mechanical Engineering, Stanford University, 1982.

Appendix A

Dimensions of Tactile Sensor

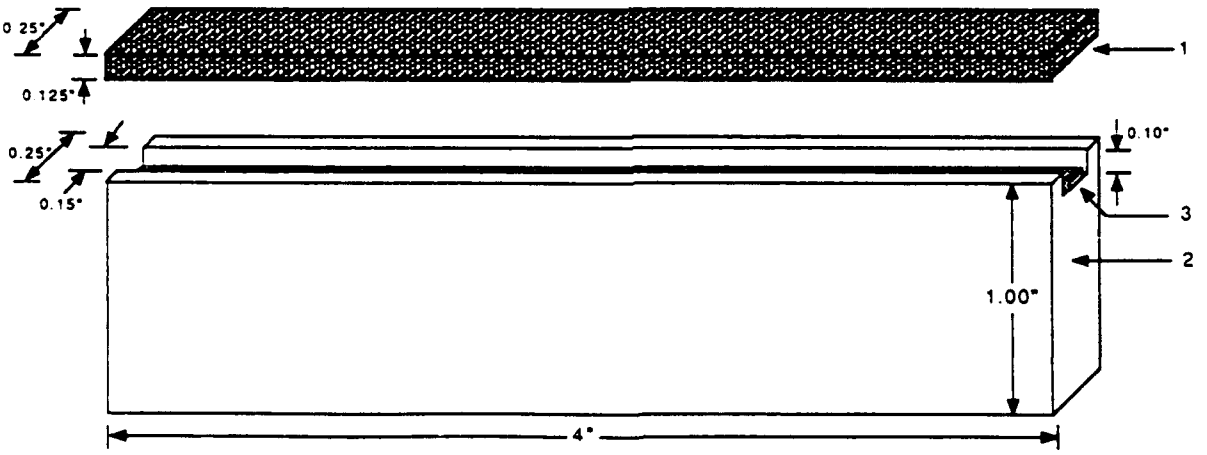

1. Insulation-conductive foam
2. Delrin Link with a milled 0.1" by 0.15" groove
3. Sensing Plate-0.1" wide gold plated nickel strip

Appendix B

Control Hardware

B.1 Control System

A block diagram of the control structure is provided in B.1. The **PALM** is controlled via a C program running on an IBM AT. Computer I/O is done through an Data Translation Analog I/O Card. This card has analog output used for command to the motor amplifier, and analog inputs used to read the tactile sensors and a linear potentiometer.

B.2 Amplifier Circuit

The lowest level control consists of a current control amplifier. A schematic is provided in Figure B.2. It was found that with no filtering on the input, noise was amplified making the system unstable. Therefore, a 100 nanofarad capacitor and a 4.9 K resistor were added to provide lowpass filtering.

At first, a voltage control circuit (see Figure B.3) was constructed. It was hypothesized that this would be equivalent to current control at stall because the back EMF is zero. The current drawn by the motor is $(i = V - V_{emf})/R_m$ where i is the current, V is the supply voltage, V_{emf} is the back EMF, and R_m is the internal

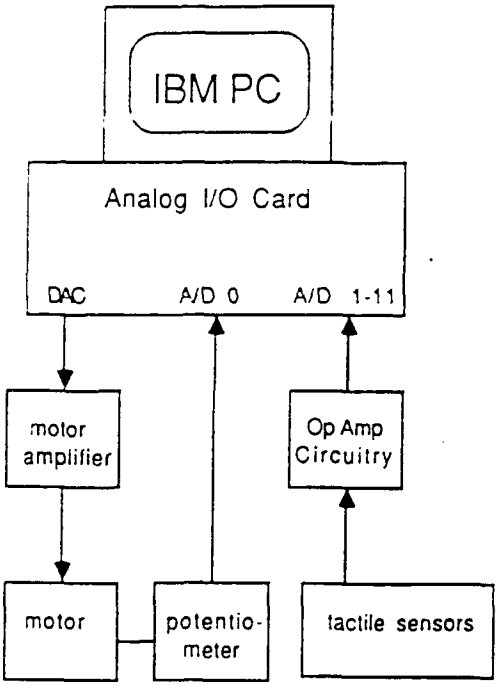

Figure B.1: Control System Block Diagram

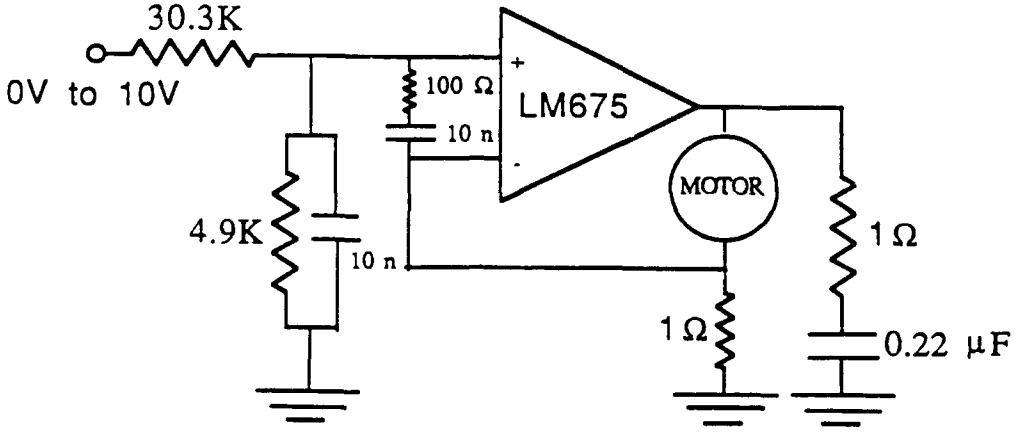

Figure B.2: Current Control Amplifier

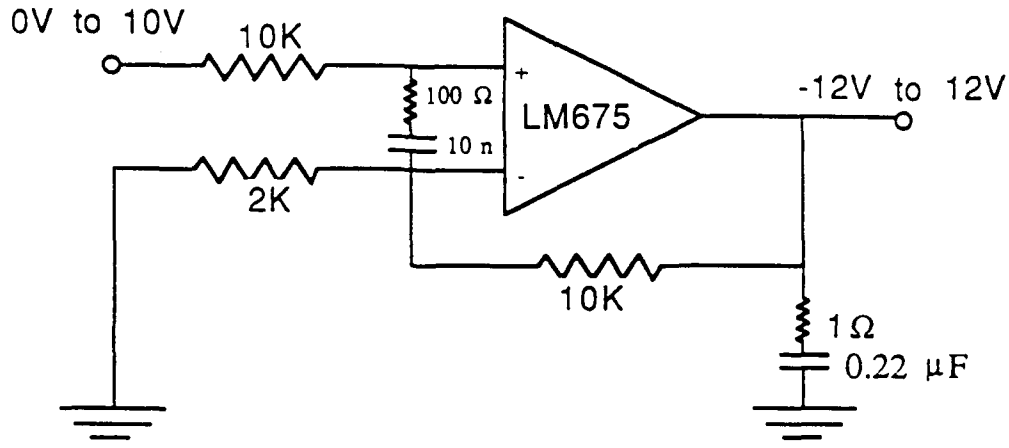

Figure B.3: Voltage Control Amplifier

resistance of the motor. It was found that the performance of this circuit was poor because the motor resistance depends on the temperature. If the motor is stalled its temperature will increase and it draws less current per volt (Figure B.4 shows the thermal dependence of the motor). The internal resistance of the motor can change by as much as 30% of the no load value when driven at the rated continuous current.

B.3 Actuator Feedback

Actuator position is measured by a linear potentiometer with a cable wrapped around the drive pulley. The advantage of a potentiometer for this application is that the Analog I/O card can access the data faster because it uses the same mode as acquiring tactile sensor readings. Another advantage is that only one wire is required instead of several digital lines Minimizing the cables running to the robot end-effector is important in most current robot designs. One disadvantages is the reduced resolution from the sensing being on the low speed side of the gear

Current (A)	Voltage (V)	Resistance (Ω)	Power (Watts)
0.25	1.49	6.0	0.37
0.50	3.12	6.2	1.56
0.75	5.54	7.4	4.16
1.00	8.13	8.1	8.13

Figure B.4: Thermal Dependence of Motor. Current is being controlled. Voltage reading is taken when steady state temperature is reached.

reduction. Another important consideration is the quality of the position signal. Noise can degrade the signal when it is run through wires over long distances. Digital signals are more tolerant to noise. One solution to this is to run all analog control and data signals in optical fibers. This, however, was beyond the scope of the thesis.